

國立臺灣大學工學院化學工程研究所



碩士論文

Department of Chemical Engineering

College of Engineering

National Taiwan University

Master Dissertation

乳酸乙酯製程之反應蒸餾系統

與不同分離組態之設計與經濟評估

Design and Economic Evaluation for Production of Ethyl  
Lactate via Reactive Distillation Combined with Various  
Separation Configurations

戴士寶

Shi-Bao Dai

指導教授：陳誠亮 博士

Advisors: Cheng-Liang Chen, Ph.D.

中華民國 107 年 6 月

June, 2018

## 誌謝



首先感謝臺灣大學程序系統工程研究室 (PSE) 陪伴我碩士班兩年生涯。謝謝指導教授陳誠亮與李豪業老師帶領菜鳥的我進入 PSE 浩瀚的研究領域；也感激兩位老師在我大學與碩班的每個學期總幫我撰寫推薦函，讓我申請獎學金更順利，幫助減輕家中負擔。同時亦感謝錢義隆與吳哲夫老師，修習老師們所開設的研究所課程，充實我更多背景知識。學長姐：小余、Mike、仕翰、惠楚、Se Li、冠辰、昆庭、于誠、傑哥、柏安、黃睿、子傑、曉玲、沅煒、Jeremy；同學：家諄、振濠、彥翔、均正、孟凱、冠霖、哲安；學弟：立軒、少秋、向璇，碩士生活因為你們而不苦悶，每天都有歡笑。

接下來感謝我求學生涯伴隨我成長的社會慈善團體：家扶基金會、中華扶輪教育基金會、漢儒文教基金會、台北北區扶輪社、儒鴻基金會、羅許基金會、法鼓山慈善基金會、青澀芷蘭菁英培育發展協會……。打從心底感激社會上有這麼多充滿愛心的團體，謝謝有您們的存在，使我無後顧之憂地專心向學。不敢說自己目前已有多大成就，但如果沒有您們這份情，我就不會是今天的我。經歷這些年，亦告訴自己未來有能力時，要懂得回饋社會中弱勢的角落，將這份情傳承。

謝謝我的好友們：韋銘、祐倫、裕意、承宣、凱聖、宛儒、水哥、廷謚、晟宇、老菊、建民、齊澤、千玉、PaPa、群祐與明旭。雖然不常見，友誼卻依然深厚著。碩班兩年，因為有你們而不孤單。

感謝命運的安排，在碩士生涯尾聲遇見我的女朋友麗珊。為了把握彼此忙碌中珍貴的時光，促使我撰寫論文與 paper 的效率開到最大。儘管未來幾年彼此有著不同人生規劃，妳還是欣賞這樣的我，願意緊握這緣份，謝謝我們的勇氣。

最後必須感謝我的母親曾慧齡女士，總是扮演著最堅實後盾在支持著我，給予我滿滿的關愛與力量。二十多年含辛茹苦提拔我至此，我想，我要好好對您說聲：「媽媽，您辛苦了！您的辛勞我皆歷歷在目。接下來的日子，您可以不必再為生計煩惱，因為有兒子在。」

「在充滿資源的環境挖掘無限可能。」儘管兩年碩班眨眼即逝，但在臺大卻獲益良多。聆聽不同類型講座與認識多元領域朋友都促使我成為更獨立的個體。謝謝臺灣大學，讓盼望飛翔的我，也能擁有一對翅膀。





## 摘要

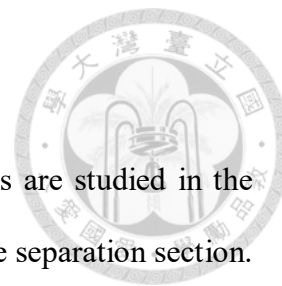
本論文針對乳酸乙酯之酯化系統，提出兩組不同生產乳酸乙酯之商業化製程。整組架構可分為反應區域以及分離區域。在適當的熱力學與動力學模型之下，先探討針對 Miller 等人<sup>1</sup>的反應區域來改善。藉由觀察反應區域第一根反應蒸餾塔塔內之各成分摩爾組成分佈，可以發現乳酸乙酯組成最高點並非出現在塔底，而是在接近塔底的板。因此在第一根反應蒸餾塔取出一股高純度乳酸乙酯側流來取代原先的產物分離塔。最後在反應段僅需兩反應蒸餾塔即可實現生產高純度乳酸乙酯之目標，其一為乳酸乙酯酯化塔，其次為水解塔進行不純物水解。

在分離區域的設計上，以兩組不同的組態－萃取蒸餾與薄膜，處理來自反應區域的水與乙醇混合物。萃取蒸餾系統在處理水與乙醇的混合物上，甘油為一相當合適的萃取劑。其原因在於比起傳統萃取劑而言，甘油提取水的效果更好。除此之外，在考量製程的綠化上，甘油為無毒化合物，因此適合作為分離水與乙醇的萃取劑。在薄膜程序上，選用商業化薄膜－PERVAP® 2201。由於來自反應區域的水含量高於薄膜操作上限，因此選用複合式的方法，先將物流送至傳統蒸餾塔進行除水，而後再由滲透蒸發程序分離乙醇與水。

程序之最適化上，以年均總成本作為目標函數，針對以上兩組製程探討不同設計與操作變數對於系統的影響以求得最佳之設計組態。結果顯示，相較於傳統的萃取蒸餾法，以滲透蒸發複合程序結合兩反應蒸餾塔製程來生產乳酸乙酯較具經濟效益。總計節省 76% 之操作成本與 31% 之年均總成本。

**關鍵字：**乳酸乙酯、程序設計、反應蒸餾、萃取蒸餾、滲透蒸發

## Abstract



Two commercial scale ethyl lactate ( $L_1E$ ) production processes are studied in the work. The  $L_1E$  processes can be divided into the reaction part and the separation section. For the reaction part, instead of the three-column design presented by Miller et al<sup>1</sup>, the proposed configuration only contains two reactive distillation (RD) columns, where the  $L_1E$  product is taken from the first RD column as a sidedraw. This novel improvement can reduce 22.26% of energy consumption in the reaction part. Additionally, disparate separation approaches such as extractive distillation (ED) and the pervaporation (PV) are then implemented to deal with the ethanol/water azeotrope. Economics for alternative configurations are analyzed to find the most competitive and cost-effective process. As a result, the RD with PV design can save at least 31.47% of total annual cost compared to the RD with ED configuration.

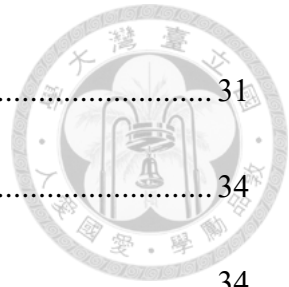
**Keywords:** Ethyl Lactate; Process design; Reactive distillation; Extractive distillation; Pervaporation.

# Contents



誌謝.....	II
中文摘要.....	IV
Abstract.....	V
1. Introduction.....	1
1.1. Review of ethyl lactate.....	1
1.2. Review of reactive distillation.....	5
1.1. Review of extractive distillation.....	8
1.2. Review of pervaporation.....	10
1.3. Literature survey.....	12
1.4. Research motivation.....	14
1.5. Dissertation organization.....	15
2. Model Building.....	16
2.1. Thermodynamic Property.....	16
2.2. Reaction Kinetics.....	22
2.3. Pervaporation Model.....	24
2.3.1. Preface.....	24
2.3.2. The influence of feed condition on membrane performance.....	26
2.3.3. Pervaporation module.....	28

2.3.4.	Pervaporation model for ethyl lactate system.....	31
3.	Steady State Design.....	34
3.1.	Preface.....	34
3.2.	Reaction Section.....	35
3.3.	Separation Section .....	40
3.3.1.	Extractive Distillation .....	43
3.3.2.	Pervaporation.....	45
3.4.	Process Optimization .....	46
3.5.	Variables in Reaction Section.....	47
3.6.	Variables in Separation Section.....	49
3.7.	Optimization Strategy.....	51
4.	Results and Discussion.....	56
5.	Conclusion .....	65
	Reference.....	66
	Appendix .....	71



## List of Figures



Figure 1-1 Typical reactive distillation column.....	7
Figure 1-2 Typical configuration of extractive distillation .....	9
Figure 1-3 The process concept by transesterification issued by Asthana et al. <sup>6</sup> .....	13
Figure 1-4 The process concept by hydrolysis issued by Miller et al. <sup>1</sup> .....	13
Figure 2-1 Binary diagram at 1 bar of ethyl lactate system .....	21
Figure 2-2 Verification of kinetic model between experimental data.....	23
Figure 2-3 The comparison between the Lumped System Method & perfect plug flow <sup>25</sup> .....	28
Figure 2-4 Systematic diagram of the Lumped System Method.....	29
Figure 2-5 The validation of the membrane model for (a) water; (b) organic .....	33
Figure 3-1 The simulation results from the process concept of Miller et al. (2010) <sup>1</sup> .....	37
Figure 3-2 The composition profile in RDC1 .....	38
Figure 3-3 The simulation results of modified process for reaction part.....	39
Figure 3-4 The optimal results for (A) RD + ED configuration; (B) RD + PV configuration.....	42
Figure 3-5 The residual curve map of EtOH/H <sub>2</sub> O/Glycerol system.....	44
Figure 3-6 Pseudo-binary vapor–liquid equilibrium for EtOH/H <sub>2</sub> O/Glycerol system <sup>30</sup> .....	44

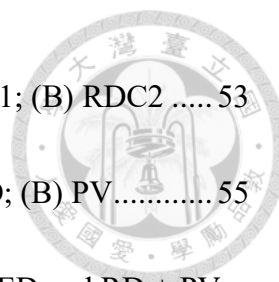


Figure 3-7 The optimization algorithm for reaction section, (A) RDC1; (B) RDC2 .....	53
Figure 3-8 The optimization algorithm for separation section, (A) ED; (B) PV.....	55
Figure 4-1 Effect of various recycled EtOH purity on TAC for RD + ED and RD + PV .....	57
Figure 4-2 Effect of various recycled EtOH purity on vacuum system cost and TAC for RD + ED.....	57
Figure 4-3 Effect of various recycled EtOH purity on membrane cost and TAC for RD + PV.....	58
Figure 4-4 Effect of total stages of C1 on the cost of ED system .....	59
Figure 4-5 Effect of EtOH purity at D3 stream on reboiler duty of C1 and required membrane area .....	61
Figure 4-6 Effect of EtOH purity at D3 stream on the cost of TAC, TIC of C1, and membrane cost .....	61

## List of Tables



Table 1-1 The major advantages of ethyl lactate <sup>2</sup> .....	3
Table 1-2 All possible reactions routes of ethyl lactate system <sup>6</sup> .....	4
Table 2-1 Source and binary interaction parameters of L <sub>1</sub> E system.....	18
Table 2-2 Ranking of azeotropic temperatures and pure component NBP temperatures	20
Table 2-3 Kinetic model for L <sub>1</sub> E system <sup>23</sup> .....	23
Table 2-4 The operating limitations of PERVAP® 2201 <sup>28</sup> .....	31
Table 2-5 Pervaporation parameters for L <sub>1</sub> E system .....	32
Table 3-1 Remaining variables in reaction section .....	48
Table 3-2 Variables for optimization for ED and PV .....	50
Table 4-1 Detailed cost distribution of RD + ED configuration.....	64



## 1. Introduction

### 1.1. Review of ethyl lactate

Ethyl lactate is a common solvent in chemical industry. The identity of this solvent is that it holds promise as a biodegradable and nontoxic replacement for petroleum-based solvents such as chlorofluorocarbons, methylene chloride, ethylene glycol ethers and chloroform that have long dominated world markets. Besides, the application of this green solvent ranges widely from coating, food, perfumery, polyurethane and pharmaceutical industry to some specific usages, for example, paint stripper and graffiti remover.<sup>2</sup> Table 1-1 lists the major advantages of ethyl lactate.<sup>2</sup>

From the economic point of view, the potential global ethyl lactate market value will rise continually to one billion US dollars in 2019.<sup>3</sup> However, the market price of ethyl lactate is almost two times higher than those traditional solvents.<sup>4</sup> This can be categorized by two reasons. Firstly, no synthetic ethyl lactate is on the market currently, which means both reactants, ethanol (EtOH) and lactic acid ( $L_1$ ) are derived from an expensive natural-based feedstock. Secondly, the cost of separation and purification of the process has been estimated to account for half of the total cost. Therefore, improvements are needed in the process of producing ethyl lactate.<sup>2,5</sup>

Ethyl lactate is usually produced through the main esterification reaction of ethanol and lactic acid. However, a key issue is that when the reactant concentration of lactic acid

is higher than 20 wt%, several types of oligomer will appear, namely dilactic acid ( $L_2$ ), trilactic acid ( $L_3$ ), and their ester ( $L_2E$ ,  $L_3E$ ). All possible reaction routes are listed in Table 1-2.<sup>6</sup> Consequently, process design definitely becomes more challenging.

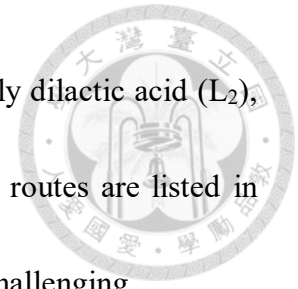
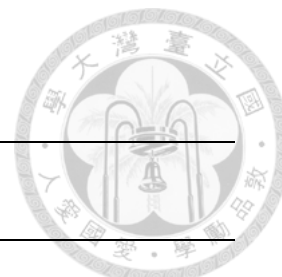


Table 1-1 The major advantages of ethyl lactate<sup>2</sup>



**Ethyl Lactate Benefits**

100% Biodegradable	Renewable – made from corn and other carbohydrates
FDA* approved as a flavour additive	EPA+ approved SNAP solvent*
Non carcinogenic	Non corrosive
Great penetration characteristics	Stable in solvent formulations until exposed to water
Rinses easily with water	High solvency power for resins, polymers and dyes
High boiling point	Easy and inexpensive to recycle
Low VOC	Not an ozone depleting chemical
Low vapor pressure	Not a hazardous air pollutant

\*U S Food and Drug Administration

+U.S. Environmental Protection Agency

\*Significant New Alternatives Policy

Table 1-2 All possible reactions routes of ethyl lactate system<sup>6</sup>

Main reaction	$L_1 + EtOH \rightleftharpoons L_1E + H_2O$	(1)
Oligomeric side reaction (a)	$L_1 + L_1 \rightleftharpoons L_2 + H_2O$	(2)
Oligomeric side reaction (b)	$L_2 + L_1 \rightleftharpoons L_3 + H_2O$	(3)
Esterification of $L_2$	$L_2 + EtOH \rightleftharpoons L_2E + H_2O$	(4)
Esterification of $L_3$	$L_3 + EtOH \rightleftharpoons L_3E + H_2O$	(5)
Transesterification of $L_2E$	$L_2E + EtOH \rightleftharpoons 2L_1E$	(6)
Transesterification of $L_3E$ (a)	$L_3E + 2EtOH \rightleftharpoons 3L_1E$	(7)
Transesterification of $L_3E$ (b)	$L_3E + EtOH \rightleftharpoons L_1E + L_2E$	(8)



## 1.2. Review of reactive distillation

Reactive Distillation (RD) is a technique which combines reaction and separation sections into a single unit thus can highly reduce the capital cost. Figure 1.1 depicts a typical reactive distillation column. In the figure, the column can be divided into three sections, the rectifying section, the reactive section, and the stripping section. In order to trigger the reaction in the column, different types of catalysts are being added. Taking an esterification reaction,  $A + B \rightleftharpoons C + D$  as an example. Two reactants, A and B are fed into the column based on the relative volatility. To be more specific, A and B represents the light and heavy components, respectively. Meanwhile, based on the Le Chatelier's Principle, high conversion and selectivity can be achieved by shifting the chemical equilibrium boundaries. Therefore, the light product, C, can be obtained from the top. On the other hand, the heavy product, D, comes out in the bottom.

Doerty and Buzard summarized the benefits of applying reactive distillation<sup>7</sup>:

- (1) Since the operation is continuously, by Le Chatelier's Principle, the system possesses a tendency of driving the reaction to the product side.
- (2) The requirement of reactant concentration in a reactive distillation column is less strict compared to traditional reactor since the products are separated continuously.
- (3) The energy input can be reduced if the reaction is an exothermic one.
- (4) Through the combination of the reactor and distillation unit in a single instrument, the

capital cost can decrease in effective amount.

(5) Conquer the limitation of the azeotrope in the system, which provides the advantage of an easier separation method.



The most common application of reactive distillation is the equilibrium reaction. Among them, the esterification reaction bears a high potential because esters have a wide range of applications in the industry. For example, compared with the traditional production route, one can save the cost up to 1/4 by utilizing reactive distillation for the production of ethyl acetate.

Despite the fact that reactive distillation provides a better choice by undergoing reaction and separation in a single unit, energy cost would still be relatively high while encountering a more complicated system. As a result, some hybrid systems are being proposed to tackle the situation. The literature study of other separation methods will be discussed in section 1.3 and section 1.4.

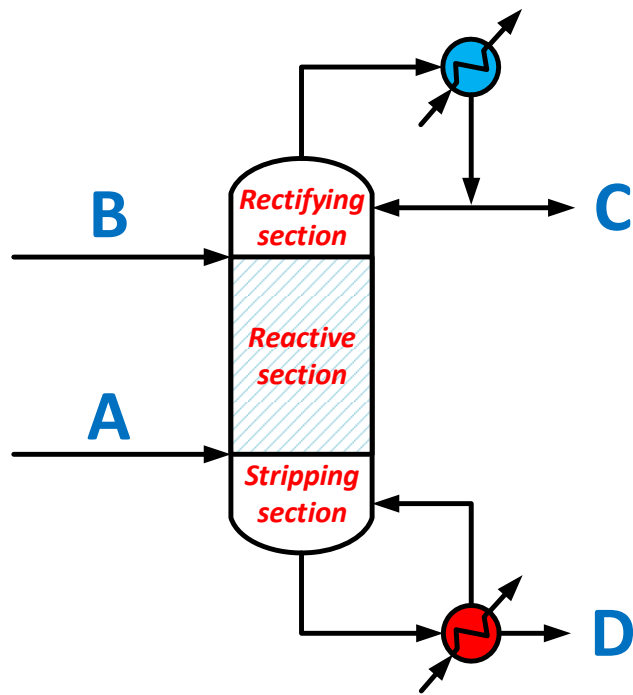


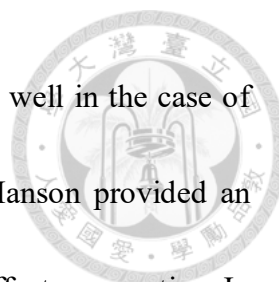
Figure 1-1 Typical reactive distillation column



### 1.1. Review of extractive distillation

Extractive distillation (ED) is a common method for breaking azeotrope. To successfully extract the component from the azeotrope, adding an additional amount of non-volatile agent, which called entrainer to the system is necessary. By altering the relative volatility, one can separate the desired product from the azeotropic mixture easily.<sup>8</sup> Figure 1.2 illustrates the typical arrangement of extractive distillation. In the figure, A+B represents the azeotrope to be separated and E is the entrainer added the system. Secondly, C1 is the extractive column to extract the target component, B; C2 is the entrainer recovery column. Normally speaking, the entrainer, E, has a higher boiling point than either A, B or A+B. Therefore, E+B and E would come out from the bottom of C1 and C2, respectively. For the propose of saving material cost, recycling of the entrainer from C2 is necessary. Since the entrainer will lose in trace amount from the system, a make-up of E should be added to maintain the overall mass balance.

There are several advantages through ED. Neither heterogeneous liquid-liquid equilibrium nor distillation boundaries are formed while introducing the entrainer. Due to the complexity of different types of azeotrope, there are many kinds of entrainer being studied to tackle with corresponding process. Weiss and Herfurth reported a paper on using ethylene glycol as a solvent for EtOH/H<sub>2</sub>O system.<sup>9</sup> Pinto et al. disclosed an idea about saline extractive distillation. In the study, compared to traditional process



(extractive and azeotropic distillation), four saline agents performed well in the case of obtaining anhydrous EtOH from fermentation broth.<sup>10</sup> Lynn and Hanson provided an uncommon process that combining extractive distillation and multi-effect evaporation. In the study, the steam consumption only took 0.94-1.47 kg per kg of EtOH product.<sup>11</sup> Arifin and Chien proposed using dimethyl sulfoxide as an entrainer to isopropyl alcohol dehydration process. While comparing with the heterogeneous azeotropic distillation, ED saves about 32.7% of TAC and 30.3% of steam cost.<sup>12</sup>

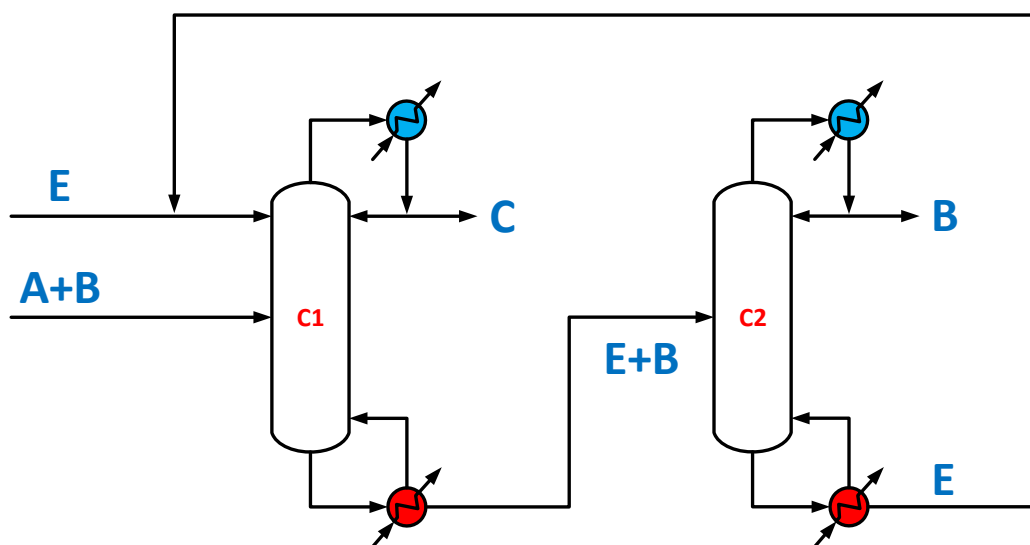


Figure 1-2 Typical configuration of extractive distillation

## 1.2. Review of pervaporation



In the current world, the idea of using energy wisely gains attention progressively. Meaning that further intensification on current processes is required. Hence, there are more and more researchers focusing on either the modification of existing processes or the development of new processes. Among them, membrane technology has been considered to be the most potential candidate. To illustrate, membrane holds various advantages. For example, it can be treated as an effective technique for separation because it is not limited by the volatility of components. Moreover, membrane unit normally requires lower energy consumption than conventional methods. Other physical properties such as high selectivity, compact and modular design are also the merits that attracting more and more value in recent years. There are numerous types of membrane. Pervaporation (PV) which firstly named by Kober in 1917<sup>13</sup> is one of the most promising alternatives among them. It refers to a process that one or more components in fluid mixture permeate through a dense membrane selectively. Despite the fact that membrane holds plenty of advantages, it still has some limitations when it comes to practical application. This is because the high capital cost and low capacity usually hinder the industry to use single membrane module directly. As a result, the most general way is to combine PV with other conventional configurations, which called PV-based hybrid process. The hybrid process provides fascinating benefits over the conventional one. One



of the pioneers studying PV-based hybrid processes was Lipnizki et al.<sup>14</sup> They give an overview of the applications, designs, and economics of the process. Since then, more and more literature that discuss the hybrid process were published. Furthermore, the integration of pervaporation with traditional esterification process is the most attractive issue among them. With constantly removing water from the system, the reaction is no longer limited by chemical equilibrium. Therefore, higher conversion can be accomplished without intensive energy consumption. Waldburger et al.<sup>15</sup> reported a paper on discussing the continuous tube membrane reactor. Compared to the traditional distillation process, the pervaporation-assisted process reduces the amount of energy requirement about 75% and 50% of total cost. Jyoti et al.<sup>16</sup> disclosed a review paper on pervaporation. In the article, various factors such as temperature, catalyst concentration, etc. are being examined fully. The authors also suggest combining PV with other reaction units to achieve high product purity. Lee et al.<sup>17</sup> proposed a process describing the esterification of ethyl acetate. Ethyl acetate, namely the desired product, is firstly side-drawing from the RD column and successively fed to the pervaporation module. The optimal design of the hybrid process saves 13% of energy compared to the two-columns process.

### 1.3. Literature survey



Gao et al. reported a paper on the L<sub>1</sub>E process by using single reactive distillation column. Whereas the process is on an experimental scale and the reaction kinetics only considered the main esterification of L<sub>1</sub> with EtOH.<sup>18</sup> Daengpradab et al. provided a process regarding commercial scale production of L<sub>1</sub>E, which consists one RD column and three separation columns. Nevertheless, the kinetics described in the process is also too simplified that neglected the oligomeric reactions.<sup>19</sup> Asthana et al. proposed a process concept on producing ethyl lactate as shown in Figure 1.3. The process mainly includes two RD columns, one for undergoing esterification of L<sub>1</sub>E (RDC1 in figure 1.3), another for transesterification reactions (RDC2 figure 1.3). However, transesterification is nearly impossible to achieve thus no further literature is unveiled regarding transesterification.<sup>6</sup> Miller et al. disclosed a commercial scale process concept with completed reaction kinetics to produce L<sub>1</sub>E. The major difference of this process is that the RDC2 in Figure 1.4 will undergo hydrolysis instead of transesterification. However, it required two RD columns and one product separation column in the reaction part, which costs a lot. Furthermore, they did not specify which configuration would be implemented in the downstream separation part.<sup>1</sup>

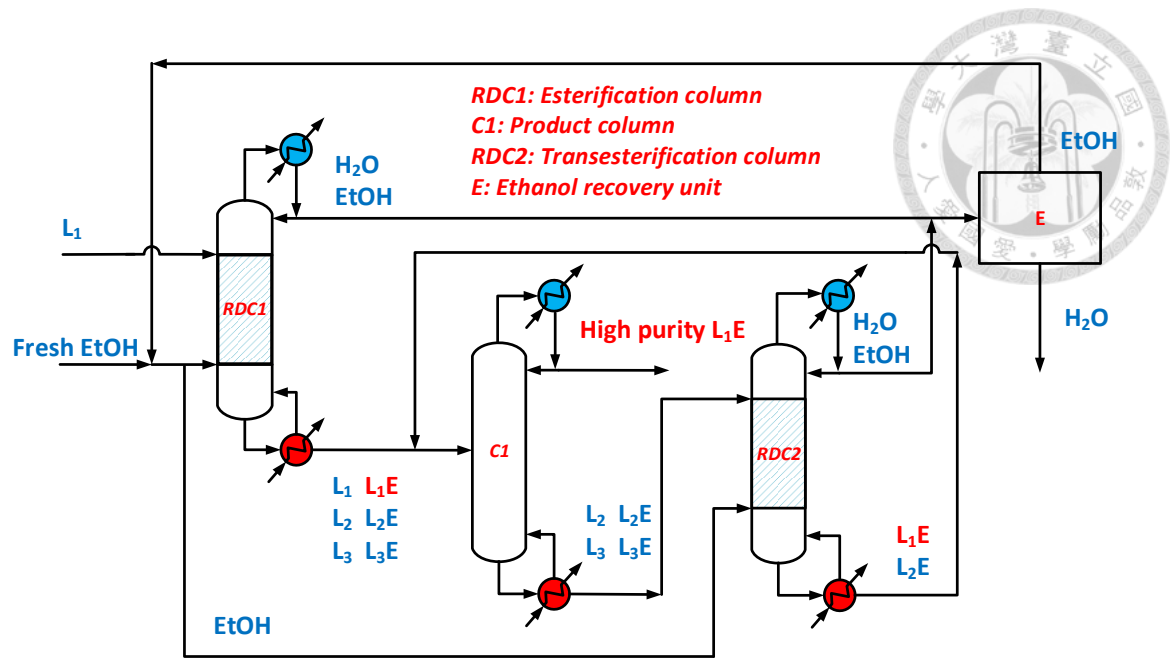


Figure 1-3 The process concept by transesterification issued by Asthana et al.<sup>6</sup>

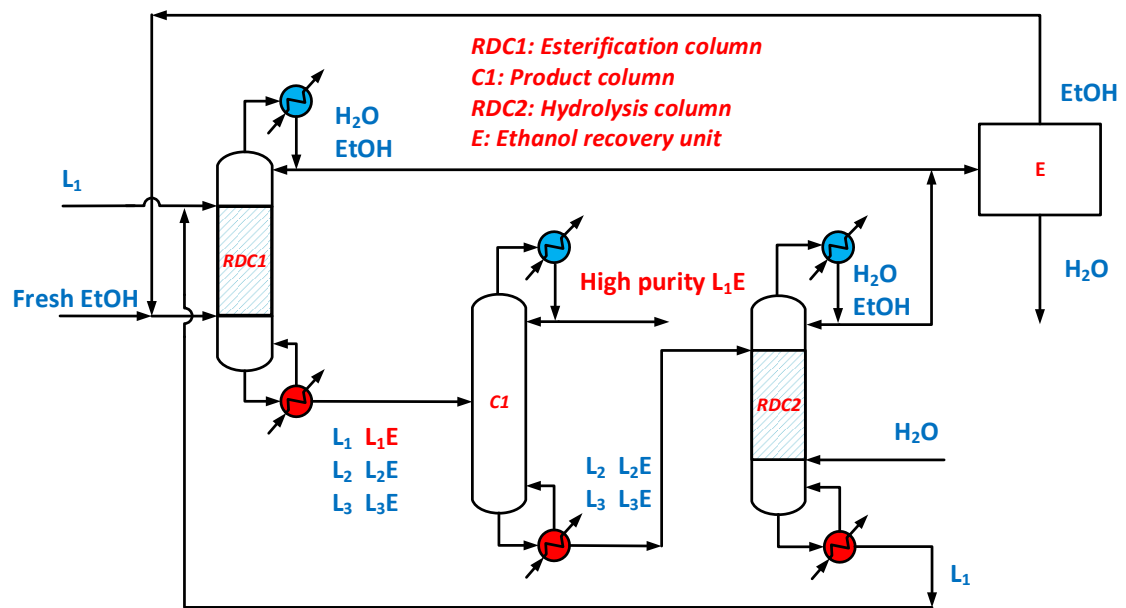
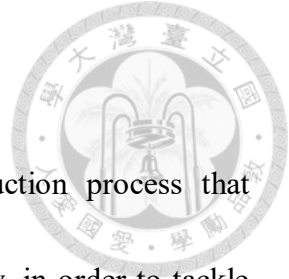


Figure 1-4 The process concept by hydrolysis issued by Miller et al.<sup>1</sup>



#### **1.4. Research motivation**

Up to this point, no commercial scale ethyl lactate production process that considering the oligomeric reactions are being studied. Additionally, in order to tackle with the downstream EtOH/H<sub>2</sub>O azeotrope, effective separation method is needed. Depending on the research done by Miller et al., the objectives of the research are as following.

- (1) Propose a complete commercial scale ethyl lactate production process with the consideration of oligomerization in the system.
- (2) Reduce the number of columns in reaction part to save energy.
- (3) Implement cost-effective separation configuration.

## 1.5. Dissertation organization

This thesis focus on the steady state design of economical plant-wide ethyl lactate production process. The overall work can be categorized into 5 cahpters:

Chapter 1 – Introduction: introduction of ethyl lactate, reactive distillation, pervaporation, literature survey, and research motivation.

Chapter 2 – Model Building: thermodynamic, reaction kinetic, and pervaporation model building of the whole system.

Chapter 3 – Steady state design: designing the process based on the thermodynamic properties, kinetic, and pervaporation model in chapter 2. The design will be discussed into two parts: the reaction section and the separation section. Then, economic analysis for various configurations are being studied to figure out the most cost-effective design.

Chapter 4 – Results and Discussion: Discussion of the optimal results based on the various design variables.

Chapter 5 – Conclusion





## 2. Model Building

### 2.1. Thermodynamic Property

Distillation is achieved through the difference of relative volatility of each components.

Accurate thermodynamic model should be carefully chosen to account for the vapor-liquid equilibrium (VLE) and vapor-liquid-liquid equilibrium (VLLE) in the system.

There are two types of thermodynamic models that can be used to describe the phase equilibrium, the Equation of State and the Activity Coefficient Model. The NRTL (Non-Random Two Liquid) model, which listed in equation 2-1, is being used in the research.

$$\ln \gamma_i = \frac{\sum_{j=1}^{nc} \tau_{ji} G_{ji} x_j}{\sum_{k=1}^{nc} G_{ki} x_k} + \sum_{j=1}^{nc} \frac{x_j G_{ij}}{\sum_{k=1}^{nc} G_{kj} x_k} \left[ \tau_{ij} - \frac{\sum_{k=1}^{nc} x_k \tau_{ki} G_{kj}}{\sum_{k=1}^{nc} G_{kj} x_k} \right]$$

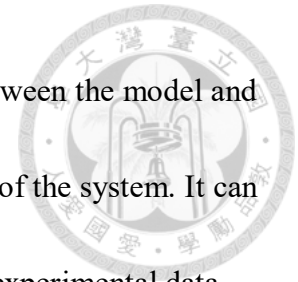
$$G_{ij} = \exp(-\alpha_{ij} \tau_{ij}), \tau_{ij} = a_{ij} + \frac{b_{ij}}{T}, \alpha_{ij} = c_{ij}, G_{ii} = 1, \tau_{ii} = 0 \quad (2-1)$$

As for the vapor phase, the second virial coefficients of Hayden -O'Connell<sup>20</sup> listed in equation 2-2 is used to fully consider the dimerization and trimerization of lactic acid in the vapor phase.

$$Z_m = 1 + \frac{B}{RT}, B = \sum_i \sum_j x_i x_j B_{ij} \quad (2-2)$$

Table 2-1 shows the source and the binary interaction parameters in the ethyl lactate system. While the parameters could not found in the built-in Aspen database, the UNIFAC functional group contributions and the Dortmund method are being used to estimate the parameters. Based on the model above, Table 2-2 lists the comparison of normal boiling

point (NBP) of pure components and the azeotropic temperature between the model and the experimental data. Figure 2-1 shows the binary diagram at 1 bar of the system. It can be found that the NRTL-HOC model is in good agreement with the experimental data.



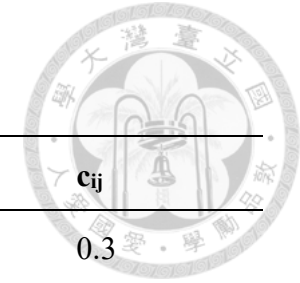


Table 2-1 Source and binary interaction parameters of L<sub>1</sub>E system

Component 1	Component 2	Source	$a_{ij}$	$a_{ji}$	$b_{ij}$ (K)	$b_{ji}$ (K)	$c_{ij}$
<b>L<sub>1</sub></b>	<b>EtOH</b>	UNIFAC	0	0	13.3045	30.4187	0.3
	<b>L<sub>1</sub>E</b>	UNIFAC	0	0	382.505	-287.146	0.3
	<b>H<sub>2</sub>O</b>	UNIFAC	0	0	-363.348	823.798	0.3
	<b>L<sub>2</sub></b>	UNIFAC	0	0	199.205	-130.146	0.3
	<b>L<sub>3</sub></b>	UNIFAC	0	0	-433.467	618.048	0.3
<b>EtOH</b>	<b>L<sub>1</sub>E</b>	UNIFAC	0	0	343.39	-233.071	0.3
	<b>H<sub>2</sub>O</b>	Aspen built-in	-0.8009	3.4578	246.18	-586.081	0.3
	<b>L<sub>2</sub></b>	UNIFAC	0	0	342.207	-248.824	0.3
	<b>L<sub>3</sub></b>	UNIFAC	0	0	753.472	-412.698	0.3
<b>L<sub>1</sub>E</b>	<b>H<sub>2</sub>O</b>	UNIFAC	0	0	-260.95	1179.05	0.3
	<b>L<sub>2</sub></b>	UNIFAC	0	0	-632.572	1091.56	0.3
	<b>L<sub>3</sub></b>	UNIFAC	0	0	-361.803	494.394	0.3
<b>H<sub>2</sub>O</b>	<b>L<sub>2</sub></b>	UNIFAC	0	0	1326.35	-404.623	0.3

	<b>L<sub>3</sub></b>	UNIFAC	0	0	1458.93	-448.795	0.3
<b>L<sub>2</sub></b>	<b>L<sub>3</sub></b>	UNIFAC	0	0	81.8535	-209.336	0.3

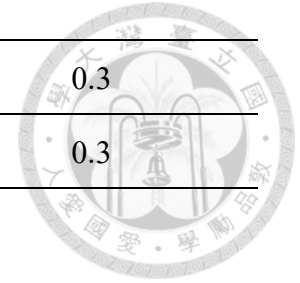


Table 2-2 Ranking of azeotropic temperatures and pure component NBP temperatures

	Experimental		Model Prediction	
	Composition	Temp. (°C)	Composition	Temp. (°C)
<b>H<sub>2</sub>O/ EtOH</b>	(0.106/0.894)	78.12	(0.112/0.888)	78.12
<b>EtOH</b>	-	78.31	-	78.29
<b>H<sub>2</sub>O/L<sub>1</sub>E</b>	N/A	N/A	(0.969/0.031)	99.85
<b>H<sub>2</sub>O</b>	-	100.00	-	100.02
<b>L<sub>1</sub>E</b>	-	154.00	-	154.49
<b>L<sub>1</sub>/L<sub>2</sub></b>	N/A	N/A	(0.404/0.596)	215.38
<b>L<sub>2</sub></b>	-	N/A	-	215.88
<b>L<sub>1</sub>*</b>	-	122.00	-	124.60
<b>L<sub>3</sub></b>	-	N/A	-	345.90

\*Measured at 15 mmHg

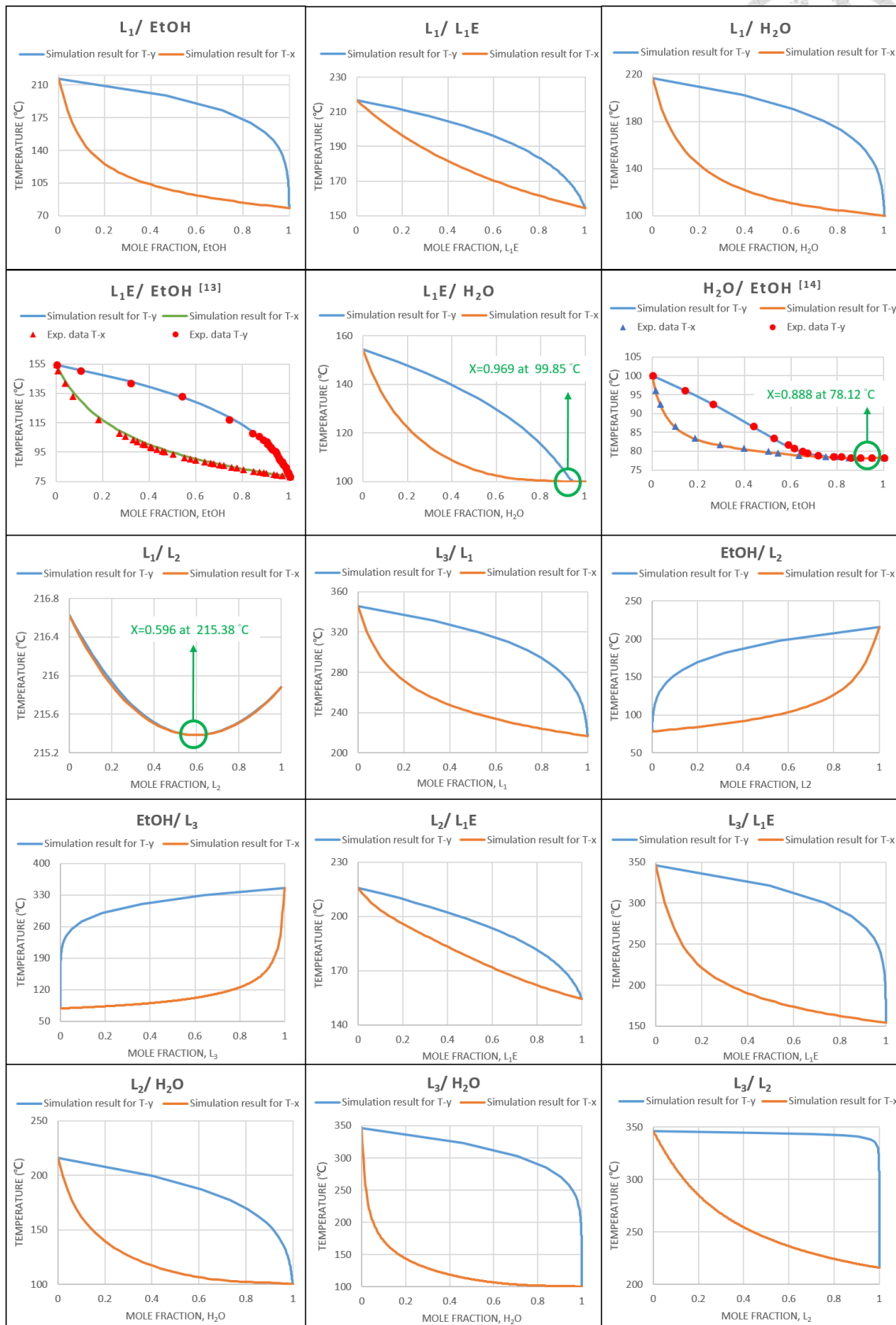


Figure 2-1 Binary diagram at 1 bar of ethyl lactate system

## 2.2. Reaction Kinetics



Although the reaction routes of the L<sub>1</sub>E system seems to be complicated, some methodology can be applied to further simplify the system. According to the research done by Asthana et al.<sup>21</sup>, since the equilibrium constants of equations (4) and (5) are relatively smaller than others, only trace amount of L<sub>2</sub>E and L<sub>3</sub>E are found. Besides, no literature is being reported to support transesterification routes (Eq.s (6) to (8)). In conclusion, equations (1) to (3) are enough to represent the system. The kinetic parameters from Su et al.<sup>22</sup> are provided in Table 2-3. For this system, Amberlyst 15 is used as the catalyst. It should be noticed that this reaction kinetic model is catalyst-weight-based ( $m_{cat}$ ). Thus, the conversion of tray volume between catalyst weight is necessary. One can solve by assuming that the solid catalyst occupies 50% of the liquid holdup in RD column trays and the density of the catalyst is 770 kg/m<sup>3</sup>. Figure 2-2 shows the verified results of the kinetic model. Solid lines and different symbols represent the simulation results and experimental data, respectively.

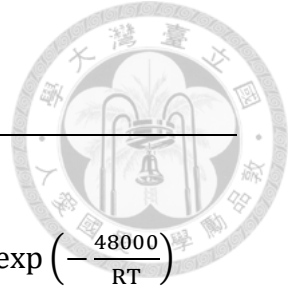


Table 2-3 Kinetic model for L<sub>1</sub>E system<sup>22</sup>

$$r_{L_1E} = m_{cat}(k_{f, L_1E}x_{L_1}x_{EtOH} - k_{r, L_1E}x_{L_1E}x_{H_2O})$$

$$k_{f, L_1E} = 6.52 \times 10^3 \exp\left(-\frac{48000}{RT}\right) \quad k_{r, L_1E} = 2.72 \times 10^3 \exp\left(-\frac{48000}{RT}\right)$$

$$r_{L_2} = m_{cat}(k_{f, L_2}x_{L_2}x_{L_1} - k_{r, L_2}x_{L_2}x_{L_2})$$

$$k_{f, L_2} = 1.10 \times 10 \exp\left(-\frac{52000}{RT}\right) \quad k_{f, L_2} = 5.54 \times 10 \exp\left(-\frac{52000}{RT}\right)$$

$$r_{L_3} = m_{cat}(k_{f, L_3}x_{L_2}x_{L_1} - k_{r, L_3}x_{L_3}x_{H_2O})$$

$$k_{f, L_3} = 4.56 \times 10^{-1} \exp\left(-\frac{50800}{RT}\right) \quad k_{r, L_3} = 2.28 \times 10 \exp\left(-\frac{50800}{RT}\right)$$

$r_i$  (kmol/s),  $m_{cat}$  (kg<sub>cat</sub>),  $k_i$  (kmol/(kg<sub>cat</sub>s)),  $R = 8.314$  (kJ/(kmol/K)),  $T$  (K),  $x_i$  (mole fraction)

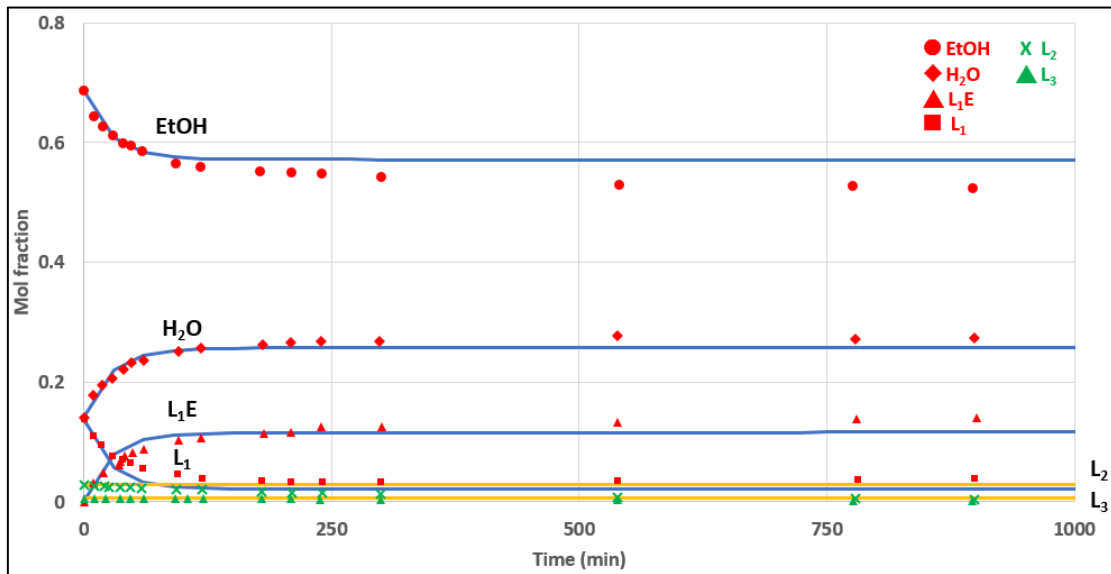


Figure 2-2 Verification of kinetic model between experimental data



## 2.3. Pervaporation Model

### 2.3.1. Preface

For the sake of simulating the pervaporation membrane, using additional software, Aspen Custom Modeler is necessary since there is no existing pervaporation module in the Aspen Plus.

There are numerous equations of phase equilibrium in the process of pervaporation. Apart from the common mass balance equation and energy balance equation, equations for component flux are also essential. Therefore, many types of equations are being studied to best describe the behavior of component flux.

The Fick's Law is most general equation to describe the flux of the component in the membrane. To be more specific, the type of the Fick's Law is the product of the diffusion coefficient and the driving force. For the diffusion coefficient, it is usually expressed by the Arrhenius equation, which affected by the temperature. In the research, the Lumped System Method by Luyben<sup>23</sup> is used to simulate the pervaporation module. Besides, the performance of the membrane is presented by two factors, the flux ( $J_i$ ,  $\text{kg}\cdot\text{m}^2\cdot\text{h}^{-1}$ ) and the separation factor ( $\alpha$ ), which defined as equation (2-3) and equation (2-4):

$$J_i = \frac{W_i}{A \times t} \quad (2-3)$$

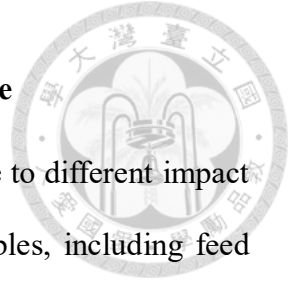
$$\alpha = \frac{\frac{y_i}{(1-y_i)}}{\frac{x_i}{(1-x_i)}} \quad (2-4)$$

where  $W_i$  is the weight of component  $i$  at permeate side (kg),  $t$  is the time interval of pervaporation ( $\text{h}^{-1}$ ),  $y_i$  and  $x_i$  represent the weight fraction of component  $i$  at permeate

side and feed side, respectively, and  $A$  is the effective membrane area ( $m^2$ ).

During the process of pervaporation, the flux is an important index for determining the quality of the membrane. Generally speaking, the flux plays an much more important role than the separation factor in the hybrid pervaporation unit. In order to obtain a higher separation efficiency, the flux should be maintained as high as possible. As a result, keeping both variables, that is, the diffusion coefficient and the driving force at higher value is reasonable. To illustrate, the driving force is provided by the vacuum pressure at the permeate side. As more and more components permeate through the membrane, the concentration of each component at the retentate side declines. Therefore, the flux decreases as a result of the declination of the driving force. This is also the reason why it is difficult for targeting the high purity product through the process since the flux is low.

Another variable for increasing the flux is the diffusion coefficient. According to the Arrhenius Equation, elevating the temperature can have positive effect on the diffusion coefficient. Consequently, it is normal to adjust the operating temperature at a higher value to increase the flux. However, as the components continuously permeate from the retentate side to the permeate side, the temperature of the stream will decrease as a result from continuous vaporization. Whereas, this will bring a negative influence on the separation function of the membrane. Accordingly, instead of using a huge membrane module, divide the membrane into several smaller units is more practical. Moreover, implement heaters between each membrane module for compensating the effect of temperature declination is feasible. Though implementing the heater would cause the cost to rise under the condition of fixed product purity, the required membrane area would reduce thus lower down the investment cost of membrane drastically.



### **2.3.2. The influence of feed condition on membrane performance**

For the pervaporation, various feed conditions would contribute to different impact on the membrane. In 2010, Anton studied a set of influential variables, including feed pressure, feed temperature, feed rate, and feed concentration on the performance of the membrane.<sup>24</sup>

The pervaporation refers to the process when the feeding liquid vaporizes through the membrane while contacting the membrane. Since the retentate side remains at liquid phase, the feed pressure has slight effect on the membrane performance.<sup>25</sup>

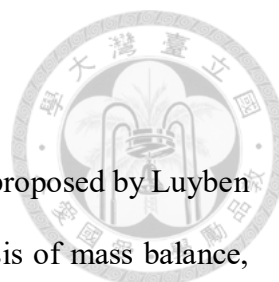
As for the feed temperature, just as discussed in section 2.3.1, while increasing the operating temperature, the diffusion coefficient would increase as a result. Hence, the flux would also rise. Nevertheless, the separation factor would decrease at the same time. The phenomenon can be originated from the reason that the diffusion coefficients of both wanted and unwanted components will be boosted while increasing the operating temperature. As a consequence, an inverse correlation will appear between the separation factor the temperature.

Thirdly, the effect of feed rate is similar to the effect of feed temperature. While increasing the feed rate, the influence of temperature declination would decrease. It is beneficial for increasing the flux through the membrane. However, the growth of the flux and the feed rate are not in proportional relation. Therefore, the product purity would contract while increasing the feed rate.

Last but not least, the pervaporation is a process of mass transfer. More specifically, the driving force rules the amount of each component transferring through the membrane. For example, increasing the product purity at the feed side also represents that the amount of unwanted components at the feed side are in small amount. As a result, the driving force is relatively small between the retentate side and the permeate side. This can also

applied to the condition that if the product purity at feed side were nearly 100%, the performance of the membrane would be disappointed.





### 2.3.3. Pervaporation module

In this research, the pervaporation model is based on the model proposed by Luyben in 2009.<sup>23</sup> With dividing the membrane into several cells, the analysis of mass balance, energy balance, and mass transfer in each section can be described successfully. This method is called Lumped System Method. The advantages of Lumped System Method is that it is convenient since we do not need to tackle with the partial differential equation as in perfect plug flow. The more cells divided in the Lumped System Method, the closer to the perfect plug flow. Figure 2-3 shows the comparison between the Lumped System Method and the perfect plug flow.<sup>24</sup>

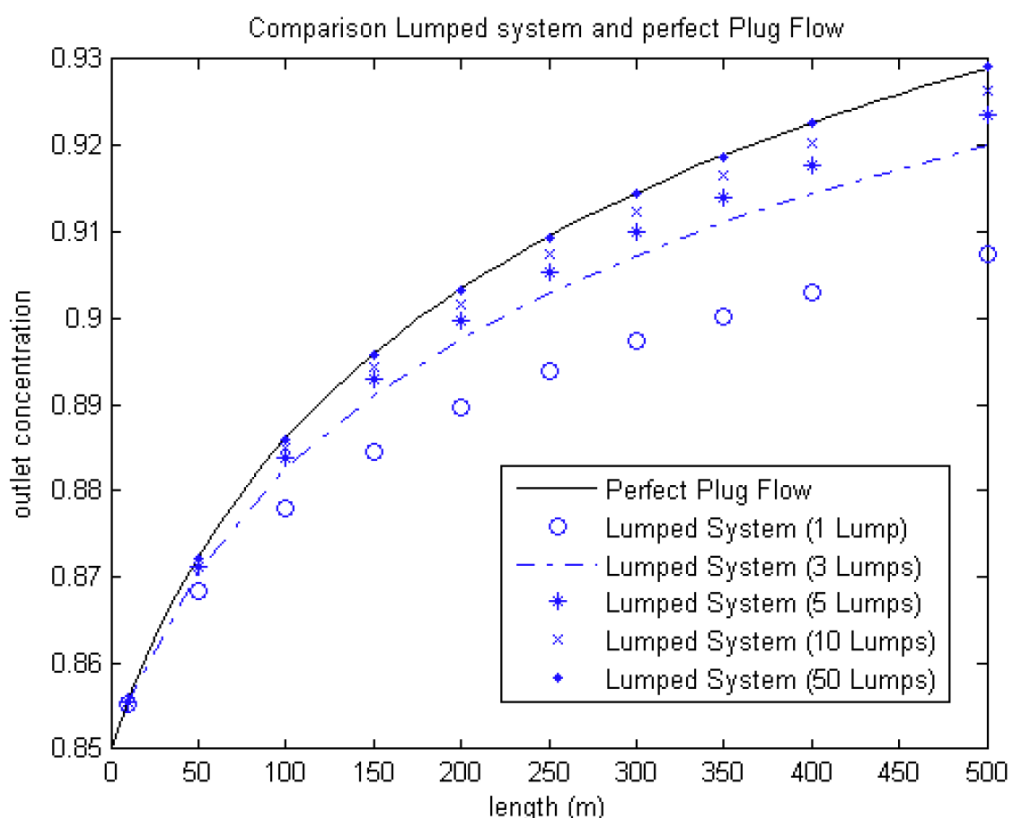


Figure 2-3 The comparison between the Lumped System Method & perfect plug flow<sup>24</sup>

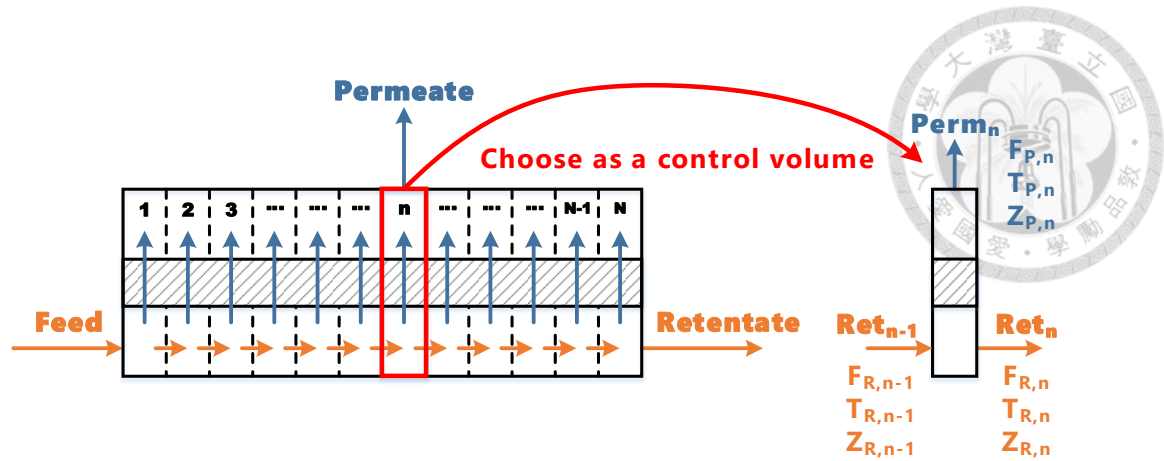


Figure 2-4 Systematic diagram of the Lumped System Method

By dividing the membrane into several small cells as shown in Figure 2-4, one can take a cell as a control volume to study the total mass balance, component balance, and energy balance as described in equation (2-5), equation (2-6), and equation (2-7), respectively:

$$\frac{dM_R}{dt} = 0 = F_{R,n-1} - F_{R,n} - F_{P,n} \quad (2-5)$$

$$M_R \frac{dZ_{R,n,i}}{dt} = F_{R,n-1} Z_{R,n-1,i} - F_{R,n} Z_{R,n,i} - F_{P,n} Z_{P,n,i} \quad (2-6)$$

$$M_R \frac{dT_{R,n,i}}{dt} = F_{R,n-1} T_{R,n-1,i} - F_{R,n} T_{R,n,i} - F_{P,n} T_{P,n,i} \quad (2-7)$$

where

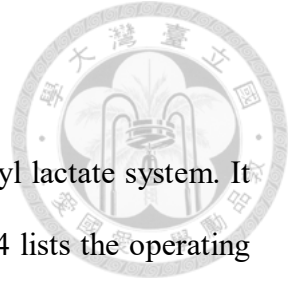
$M_R$  is the molar holdup in the membrane: different membrane area correspond to different value of  $M_R$ . The relation is that every square meter of membrane area corresponds to a hold up of  $0.003 \text{ (m}^3\text{)}^{26}$ .

$F_n$  is molar flowrate from cell  $n$ , and the subscript R and P are represented as retentate or permeate side respectively.

$z_i$  is the molar fraction for species  $i$ .

$h$  is the molar enthalpy of liquid in retentate side, and  $H$  is the molar enthalpy of vapor in permeate side.





### 2.3.4. Pervaporation model for ethyl lactate system

The membrane called PERVAP® is used for simulating the ethyl lactate system. It is a commercial membrane provided by Sulzer ChemTech. Table 2-4 lists the operating conditions of the membrane.<sup>27</sup>

Table 2-4 The operating limitations of PERVAP® 2201<sup>27</sup>

<b>The properties of PERVAP® 2201 (as reported by the manufacturer)</b>	
<b>Manufacturer: Sulzer ChemTech.</b>	
Maximum temperature (°C)	105
Maximum water content in the feed	< 50
Organic acids	< 50
pH	2-7

For the system of ethyl lactate, Delgado et al. released their study referring to the parameters of the mass transfer. The driving force is weight concentration based, which is shown in equation (2-8) and (2-9)<sup>28</sup>:

The flux of H<sub>2</sub>O:

$$J_w = k_a \exp\left(\frac{-E_D}{RT}\right) [\exp(k_b w_{w,f}) - 1] \quad (2 - 8)$$

The flux of other organic compounds:

$$J_i = k_a \exp\left(\frac{-E_D}{RT}\right) \exp(k_b w_{w,f}) w_{i,f} \quad (2 - 9)$$

where w is the concentration at the feed side, and the subscript w and i are represented as

water or organic compound, respectively (kg/kg).  $J$  is the flux crosses the membrane ( $\text{kg}\cdot\text{h}^{-1}\cdot\text{m}^{-2}$ ).

The parameters are shown in Table 2-5. It is worth to notice that the membrane is really unfavorable for organic components. Also, the feed stream to the pervaporation module composed relatively small amount of  $L_2$  and  $L_3$  in the system. Therefore, the flux of  $L_2$  and  $L_3$  can be reasonably neglected.

Table 2-5 Pervaporation parameters for  $L_1E$  system

Component	$k_a$ ( $\text{kg}\cdot\text{h}^{-1}\cdot\text{m}^{-2}$ )	$E_D$ ( $\text{kJ}\cdot\text{mol}^{-1}$ )	$k_b$ ( $\text{kg}\cdot\text{h}^{-1}\cdot\text{m}^{-2}$ )
$\text{H}_2\text{O}$	$1.19 \times 10^7$	49.96	2.17
EtOH	$4.25 \times 10^5$	51.41	8.10
$L_1E$	$1.93 \times 10^3$	40.93	9.58
$L_1$	$9.72 \times 10^8$	76.89	6.34



Figure 2-5 (a) and Figure 2-5 (b) shows the validation between the experiment and simulation results. The symbol and the line represent the experimental data and the model, respectively.

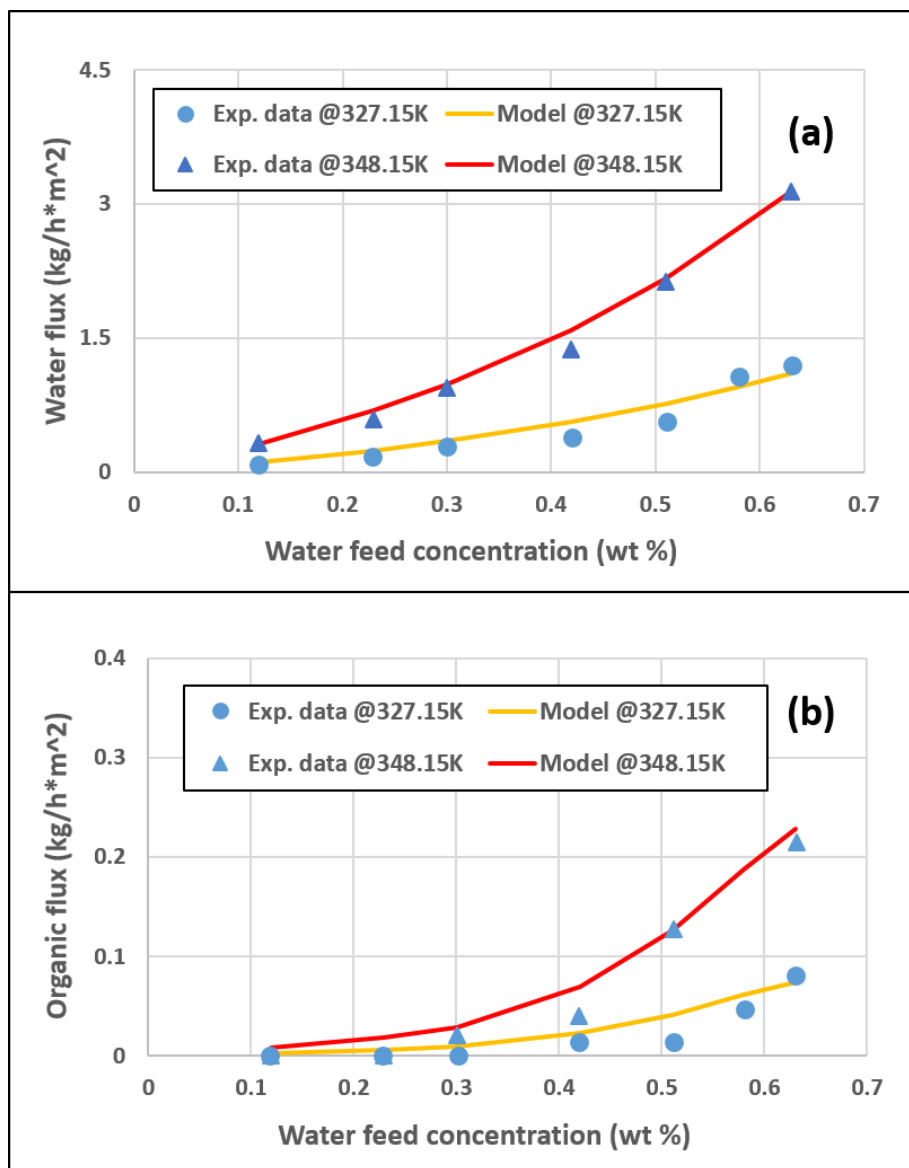


Figure 2-5 The validation of the membrane model for (a) water; (b) organic

### 3. Steady State Design

#### 3.1. Preface

The process designed here is to construct the commercial L<sub>1</sub>E production process.

The commercial simulator, Aspen Plus v9.0 is used for simulation. The membrane module for PV is developed and implemented into Aspen Plus interface via Aspen Custom Modeller. The annual L<sub>1</sub>E production rate is set as 25 million pounds (roughly as 13.88 mole/min). The specification of L<sub>1</sub>E is 0.990 (molar basis) to meet the product requirement. Besides, the purity of three feed streams, namely, EtOH, L<sub>1</sub>, and H<sub>2</sub>O are 0.900, 0.152 and 0.995 (molar basis), respectively.





### 3.2. Reaction Section

Figure 3-1 shows the base case simulation results of the reaction part from the process concept of Miller et al. (2010). It consists of two RD columns as denoted as RDC1 and RDC2 and one conventional distillation column (C1) separating L<sub>1</sub>E from the top. By analyzing the composition profile in RDC1 (Figure 3-2), we found that the highest purity of the desired product, L<sub>1</sub>E does not appear in the bottom. Instead, it arises on the 57<sup>th</sup> stage and shows the purity of 0.964 that is higher than 0.920 in the bottom stream. Therefore, it can be fairly considered to draw a side stream from the middle of RDC1 to replace C1.

Figure 3-3 shows the modified design of the reaction part. The product (L<sub>1</sub>E) is taken from the 39<sup>th</sup> stage of RDC1 as a side draw. Additionally, by changing the operating condition, such as the reboiler duty, L<sub>1</sub>E in the side draw can meet our specification of 0.990. By comparing this novel configuration with the original design, the energy has been saved for about 22.3 %.

For the further design of the process, the Mix stream from reaction section should be fairly treated. The Mix stream composes mainly of EtOH and H<sub>2</sub>O thus separating them by single distillation column is almost impossible because typical azeotrope will appear. In addition, in order to lower down the raw material cost of EtOH and H<sub>2</sub>O in reaction section, effective separation technique for treating Mix stream is necessary. As a

consequence, different separation configurations will be discussed in the following section.



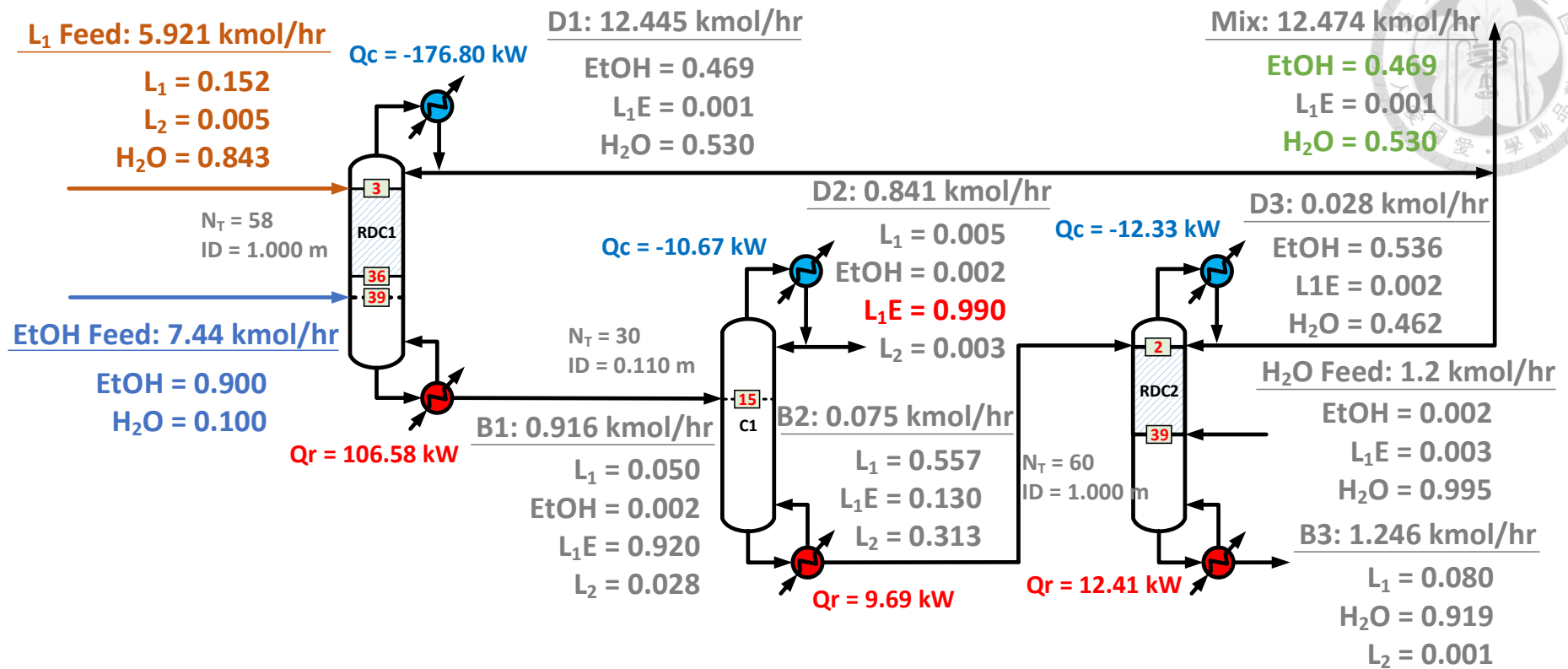
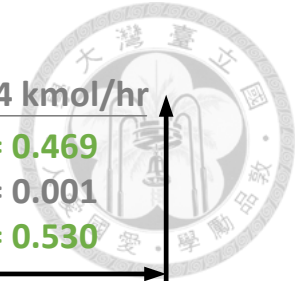


Figure 3-1 The simulation results from the process concept of Miller et al. (2010)<sup>1</sup>

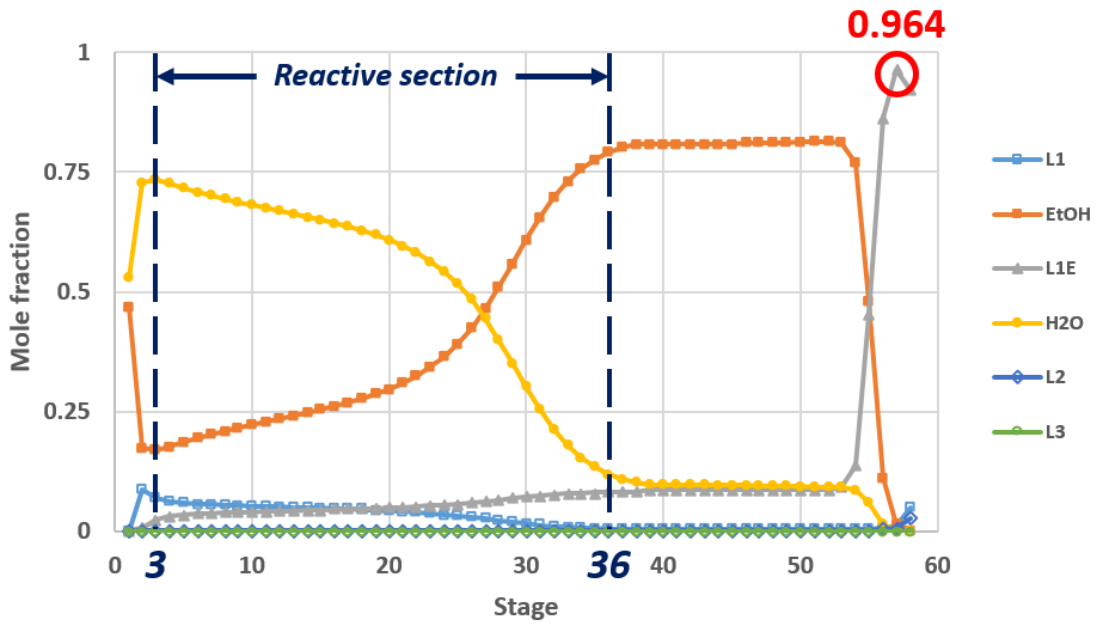


Figure 3-2 The composition profile in RDC1

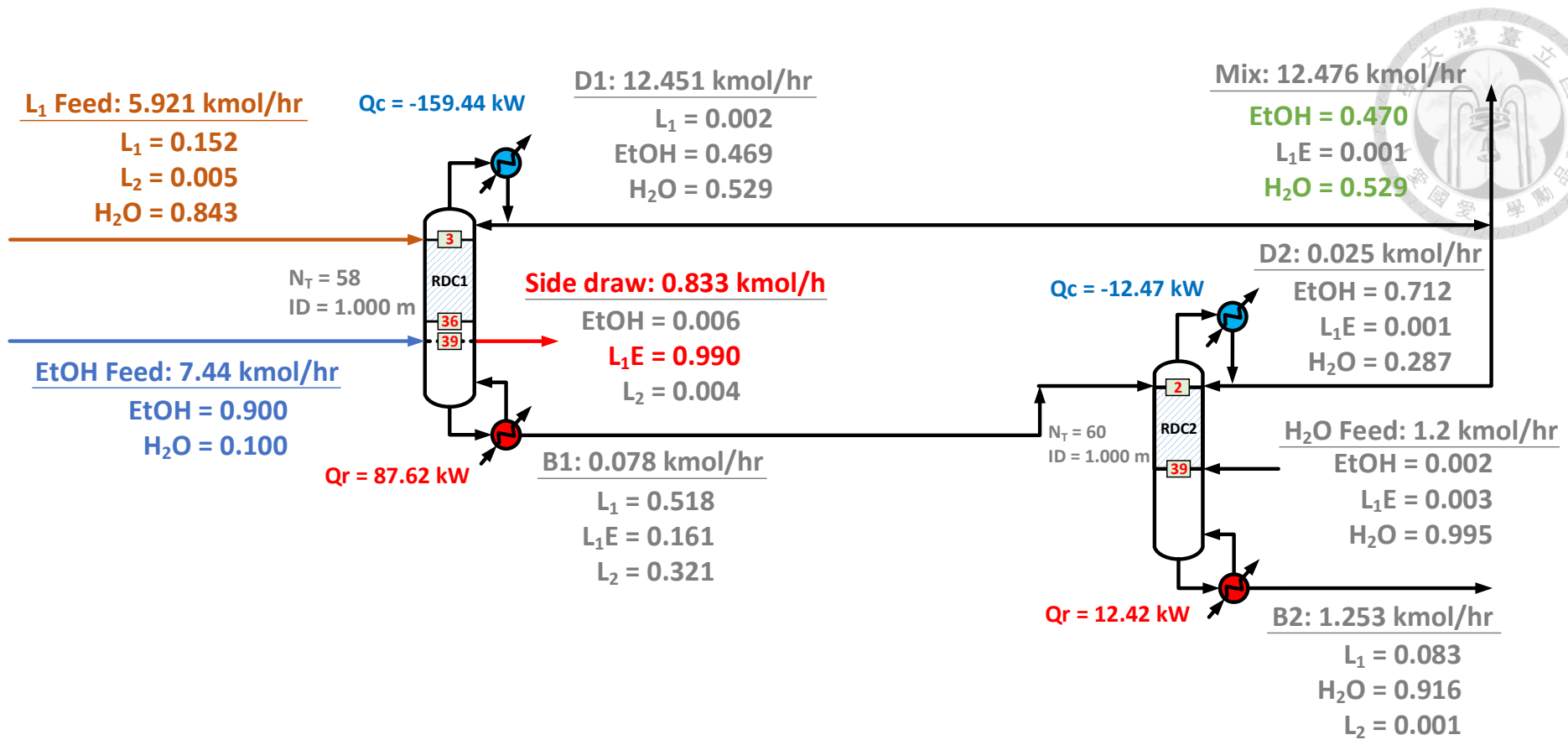
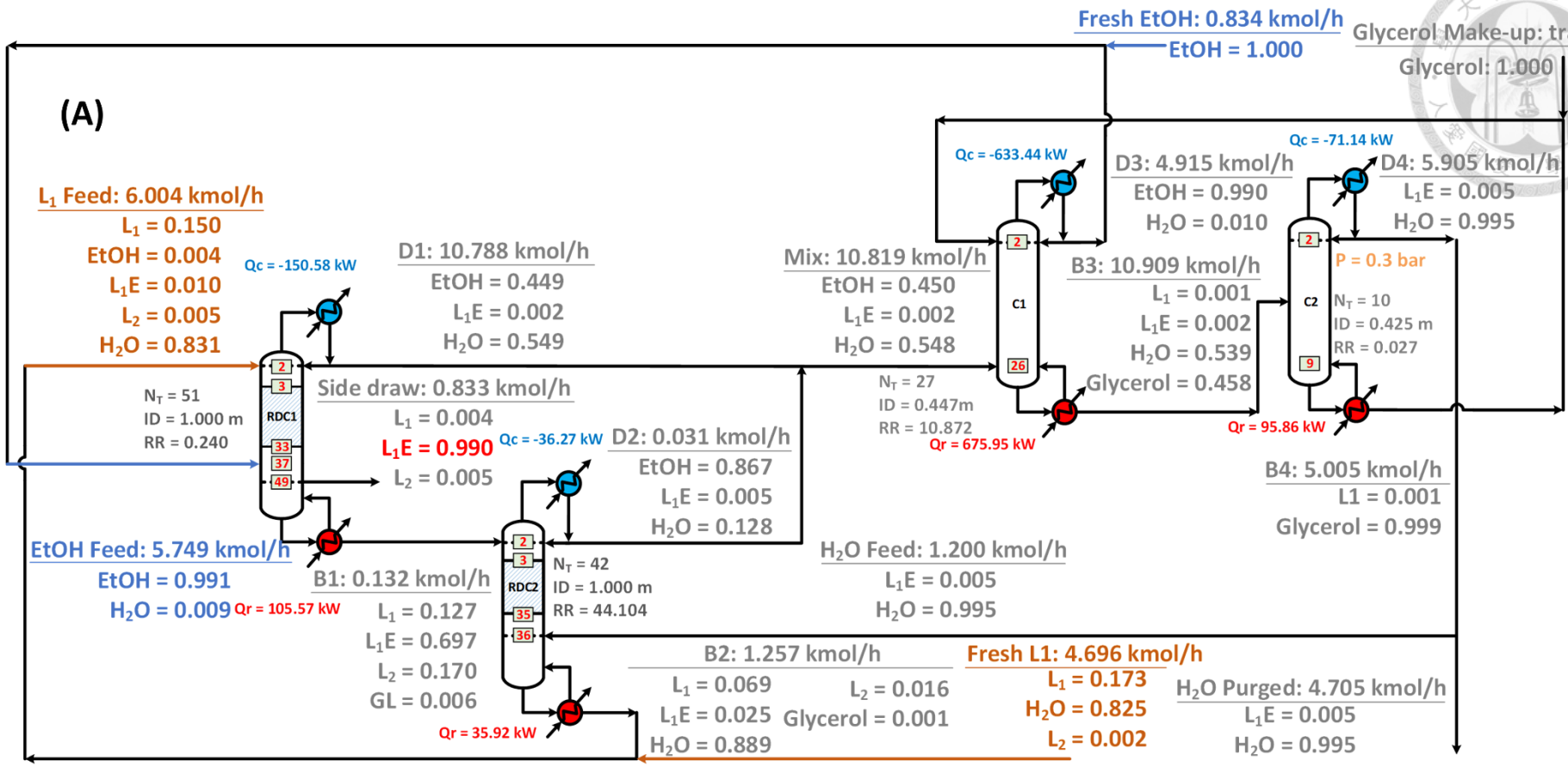
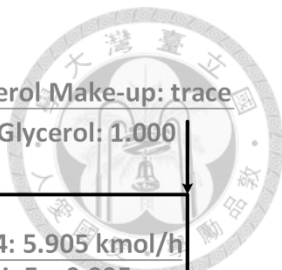


Figure 3-3 The simulation results of modified process for reaction part

### 3.3. Separation Section

In this section, two approaches of separating EtOH/H<sub>2</sub>O azeotrope will be introduced. Namely, the conventional technique called extractive distillation and the novel pervaporation method. Figures 3-4 (A) and (B) show the optimal results of RD + ED and RD + PV systems, respectively.





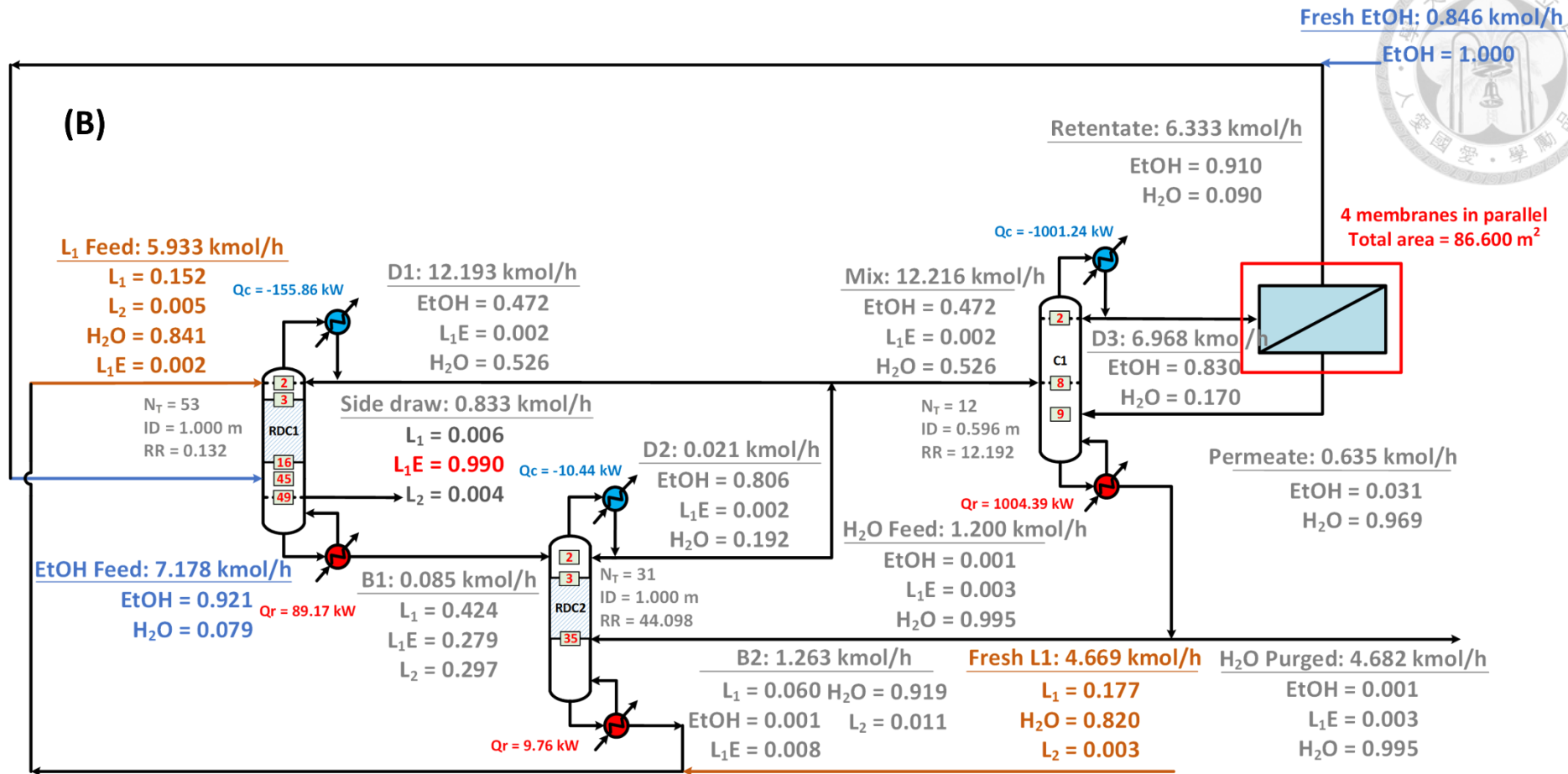


Figure 3-4 The optimal results for (A) RD + ED configuration; (B) RD + PV configuration



### 3.3.1. Extractive Distillation

For the RD + ED system, the detailed optimizing procedure will be discussed in section 3.3. The entrainer used in the extractive section is glycerol. Figure 3-5 shows the residual curve map of adding glycerol into EtOH and H<sub>2</sub>O at 1 bar. The reason of choosing glycerol is that it is non-toxic and effective in extracting EtOH from H<sub>2</sub>O. According to Lee and Pahl<sup>29</sup>, the effect of introducing glycerol can be observed from Figure 3-6, which is the pseudo-binary vapor–liquid equilibrium diagram for ethanol–water–glycerol system. Glycerol obviously eliminates the EtOH/H<sub>2</sub>O azeotrope and changes the VLE curve. Besides, one should note that glycerol is relatively sensitive to temperature. The component will crack down at 293 °C. Hence, the pressure of the entrainer recovery column (C2 in Figure 3-4 (A)) is set as 0.3 bar to ensure our design is practical. For the separation part, C1 represents the column to recycle our reactant, EtOH from the top (D3). The rest of water and entrainer will come out from B3 then fed to C2. The goal of C2 is purifying glycerol coming out at B4. Furthermore, since the boiling point of water is less than glycerol, water will come out from the top (D4). Last but not the least, because the amount of required H<sub>2</sub>O (1.200 kmol/hr) in RDC2 is less than the amount from D4 (5.905 kmol/hr), purging excess H<sub>2</sub>O is necessary.

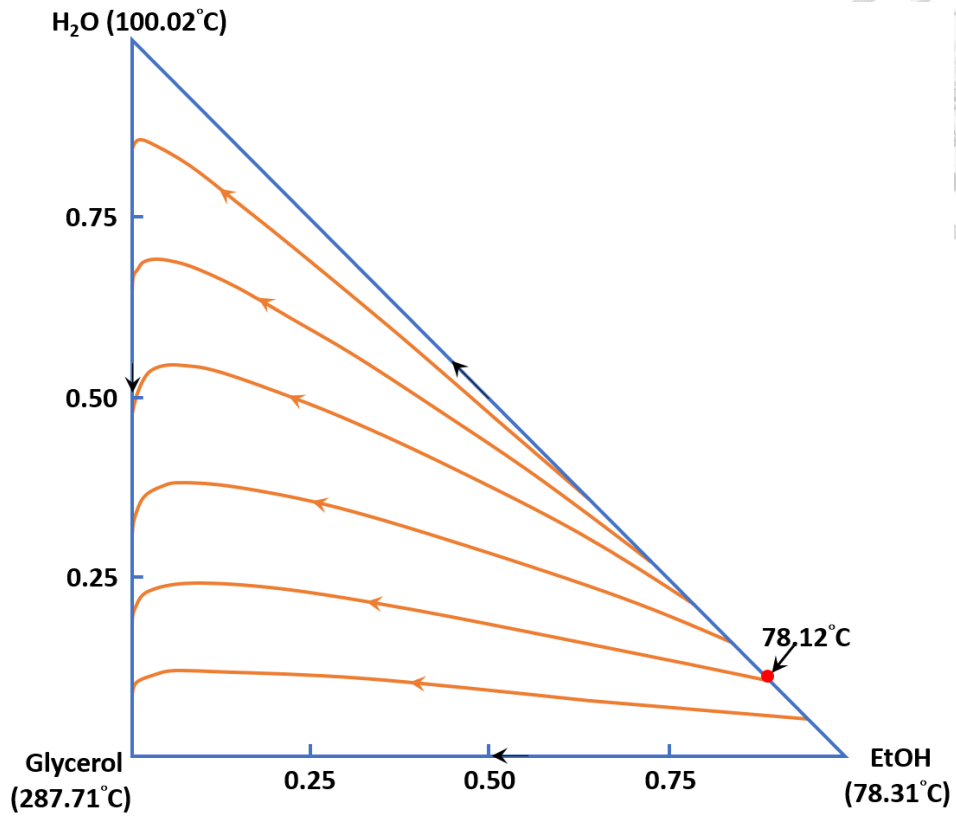


Figure 3-5 The residual curve map of EtOH/H<sub>2</sub>O/Glycerol system

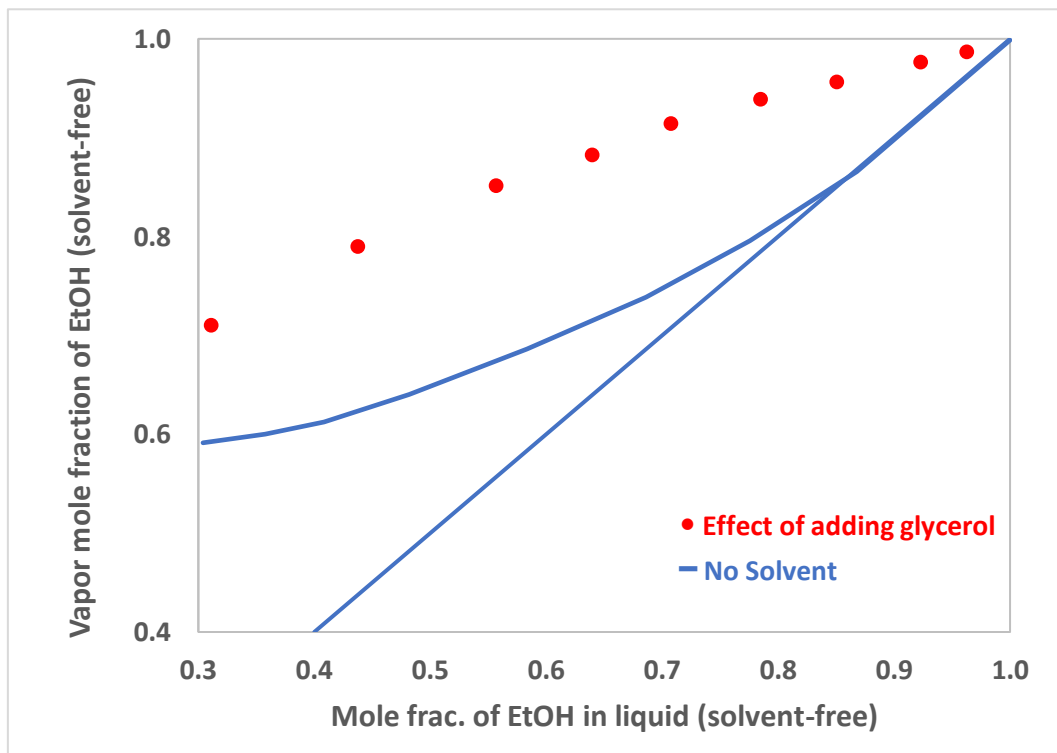
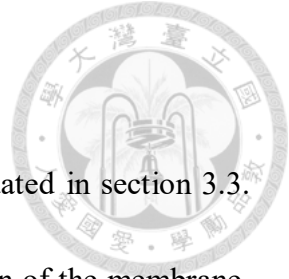


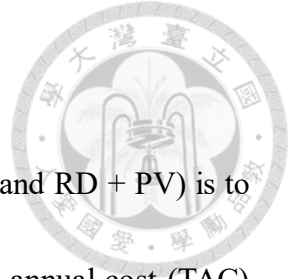
Figure 3-6 Pseudo-binary vapor-liquid equilibrium for EtOH/H<sub>2</sub>O/Glycerol system<sup>29</sup>



### 3.3.2. Pervaporation

The detailed optimizing procedure for RD + PV will be elucidated in section 3.3.

Since the H<sub>2</sub>O content in Mix exceeds the upper operating limitation of the membrane, introducing a pre-concentrator (C1 in Figure 3-4 (B)) before the pervaporation module is inevitable. The aim of the pre-concentrator is to enrich the content of EtOH in a stream. In other words, most of H<sub>2</sub>O in Mix will come out from the bottom of C1. Again, the required H<sub>2</sub>O (1.200 kmol/hr) in RDC2 is in relatively small amount, so splitting excess H<sub>2</sub>O from the bottom is essential. On the other hand, most of EtOH will come out as a distillate (D3) then sent to the membrane module. Four identical membranes are in a parallel arrangement. Each of them has the area of 21.65 m<sup>2</sup>. As reported by Lee et al.<sup>17</sup>, factor such as the composition in the feed will drastically influence the needed membrane area. Accordingly, arranging in a parallel way of this special type of membrane needs less area than series arrangement. Because the membrane is preferably water-permeable, the retentate side comprises mostly of EtOH, which can be recycled back to RDC1 as a reactant. Diversely, the rest of EtOH and a majority amount of H<sub>2</sub>O will constitute the permeate side, which will be sent back to C1 for further purification.



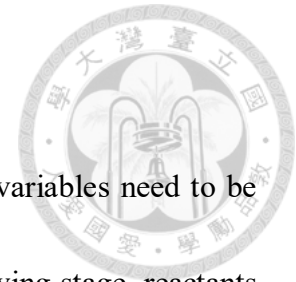
### 3.4. Process Optimization

The objective of optimization for these two process (RD + ED and RD + PV) is to identify which one is much more economical-competitive. The total annual cost (TAC) analysis is used in this study. The function of calculating TAC is shown in equation (3-1), which is a combination of annual operating cost (AOC) and annualized total capital cost (TCC).

$$\text{TAC} = \text{AOC} + \frac{\text{TCC}}{\text{payback period}} \quad (3 - 1)$$

The payback period is set as 8 years in this study. The reason for choosing 8 instead of 3 years is that in real-world industry, 8 years is more practical. The calculation for column and heat exchanger as provided in Appendix is based on Douglas<sup>30</sup>. The piping and pumping cost are ignored for the analysis. The membrane price is taken from Van Hoof et al.<sup>31</sup>, and the lifetime of the membrane is assumed as 3 years. Furthermore, the cost of the membrane is composed of two parts: the membrane material with cost per area and the membrane modules with cost per unit.<sup>24</sup> The capital and operating cost of the vacuum system are based on Woods<sup>32</sup> and Oliveira et al.<sup>33</sup>, respectively. As for the vacuum cost of the ED system, the calculation is rooted on Seider et al.<sup>34</sup> Eventually, all variables are divided into two parts for subsequent discussion.

### 3.5. Variables in Reaction Section

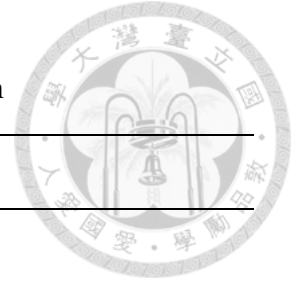


In optimizing RDC1 in the reaction section, there are several variables need to be classified, including column pressure, side draw flow rate, side-drawing stage, reactants feed ratio, reactants feed stages, and number of trays in rectifying, reactive, and stripping section. As for RDC2, most of the variables are the same as RDC1 except for side-drawing stage since no side draw is presented in the column. Next, some assumptions are being made to simplify our procedure:

- (1) The column is operated under normal pressure while cooling water can be used.
- (2) The flow rate of side draw is fixed as 0.833 kmol/h to meet the requirement of product volume and the product specification.

Finally, the remaining variables in the reaction section are listed in Table 3-1.

Table 3-1 Remaining variables in reaction section



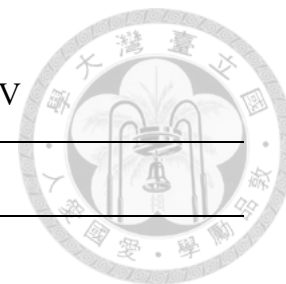
Column	Variables
<b>RDC1</b>	sidedrawing stage ( $N_{L1E}$ ); EtOH/ $L_1$ feed ratio ( $FR1$ ); $L_1$ feed stage ( $F_{L1}$ ); EtOH feed stage ( $F_{EtOH}$ ); number stages of enriching, reactive, stripping section ( $N_{En1}$ , $N_{R1}$ , and $N_{S1}$ )
<b>RDC2</b>	EtOH/ $L_1$ feed ratio ( $FR2$ ); $H_2O$ feed stage ( $F_{H2O}$ ); B1 feed stage ( $F_{B1}$ ); number stages of enriching, reactive, stripping section ( $N_{En2}$ , $N_{R2}$ , and $N_{S2}$ )

### 3.6. Variables in Separation Section



To discuss variables in the separation section, we will discuss the ED system first, then investigate the PV system. In the ED system, there are two columns, namely C1 and C2. The feed ratio of GL/Mix will directly affect the cost of C1 because the more glycerol introduced to the column the more energy is needed for separation. Also, the amount of glycerol will influence the duty applied in C2. Hence, for optimizing the ED system, one must lump C1 and C2 together for full consideration. As for the PV system, the EtOH purity at D3 will not only have the impact on the cost of C1, it likewise affects the membrane area. To illustrate, while choosing a higher purity of EtOH at distillate, smaller membrane area is required and vice versa. Besides, the inlet temperature to the membrane is fixed as 95 °C to prevent exceeding the upper operating limitation<sup>27</sup>. The permeate side pressure is kept at 0.16 bar.<sup>24</sup> According to Tusel and Brüscke<sup>25</sup>, the variation of inlet pressure does not have a significant effect. Therefore, the inlet pressure is set as 5 bar to avoid vaporization of D3 at 95 °C. Table 3-2 indicates the overall variables needed to be optimized for both ED and PV system.

Table 3-2 Variables for optimization for ED and PV

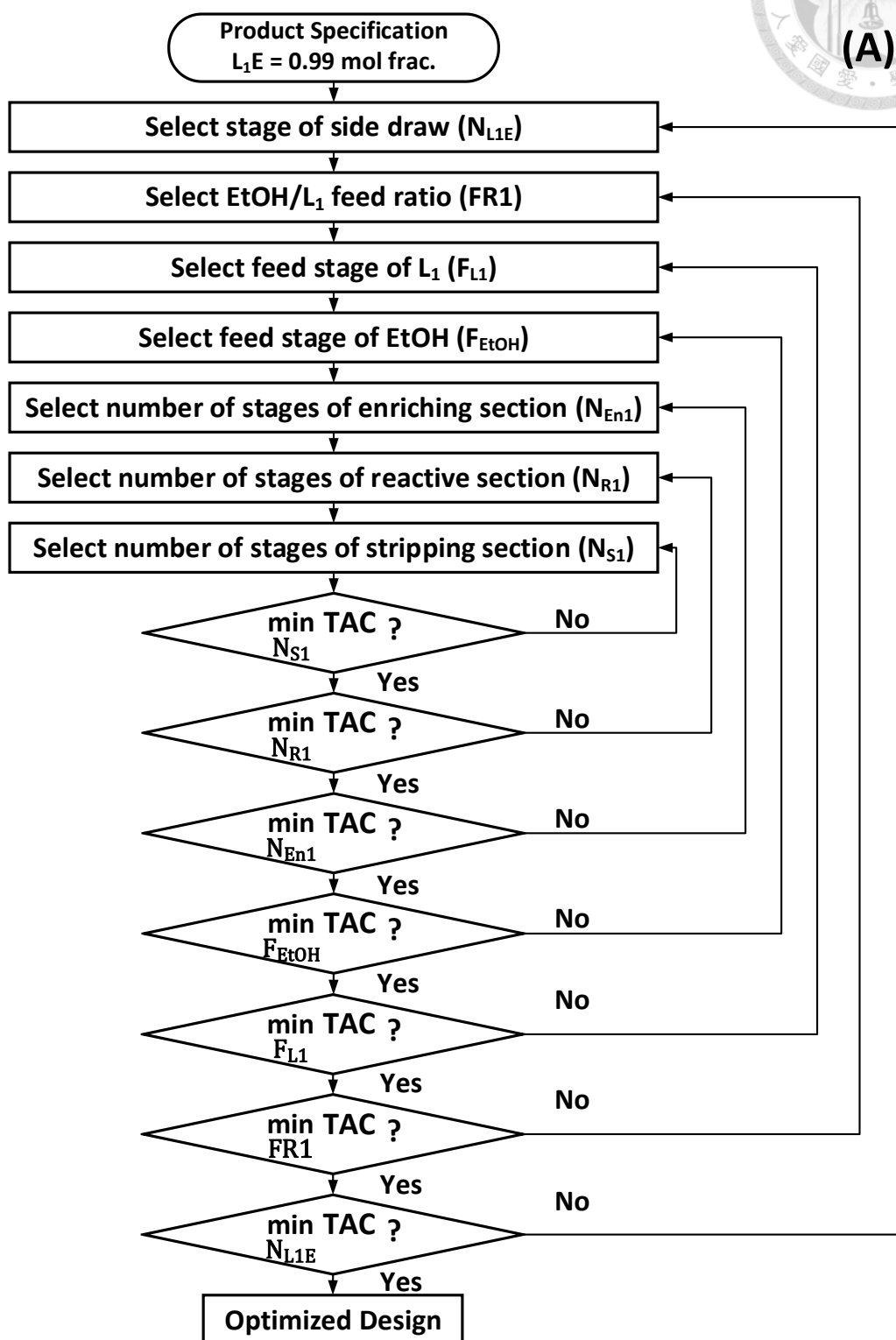


System	Variables
ED	GL/Mix feed ratio ( $FR_3$ ); Mix feed stage ( $F_{Mix}$ ); GL feed stage ( $F_{GL}$ ); C1 total stages ( $N_{T1}$ ); B3 feed stage ( $F_{B3}$ ); C2 total stages ( $N_{T2}$ )
PV	EtOH purity at D3 ( $X_{Et}$ ) and corresponding membrane area ( $A_{mem}$ ); Mix feed stage ( $F_{Mix}$ ); permeate feed stage ( $F_P$ ); C1 total stages ( $N_{T1}$ )

### 3.7. Optimization Strategy

The design procedure follows the direct search method proposed by Hooke and Jeeves.<sup>35</sup> During the optimization, sensitivity test for the design and control variables can be recorded and make the researchers easily understand the effect of these variables on the process. The direct search method can be applied to most processes which are simulated by some commercial simulators such as Aspen Plus. For the reaction section, Figure 3-7 (A) and Figure 3-7 (B) represent the algorithm for optimization for RDC1 and RDC2, respectively. For the separation section, Figure 3-8 (A) and Figure 3-8 (B) represent the algorithm for optimization of ED and PV, respectively.





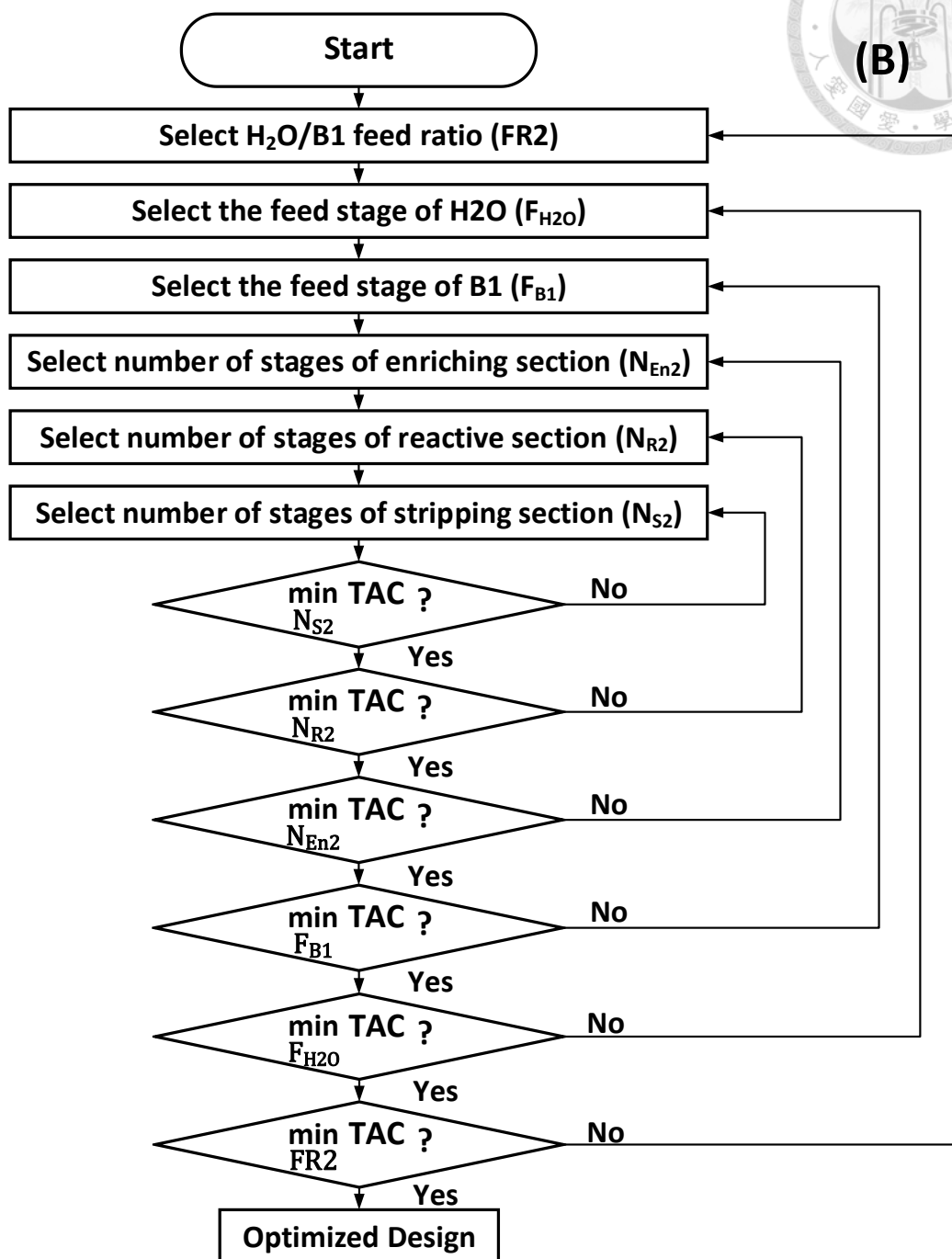
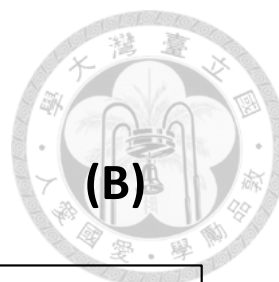
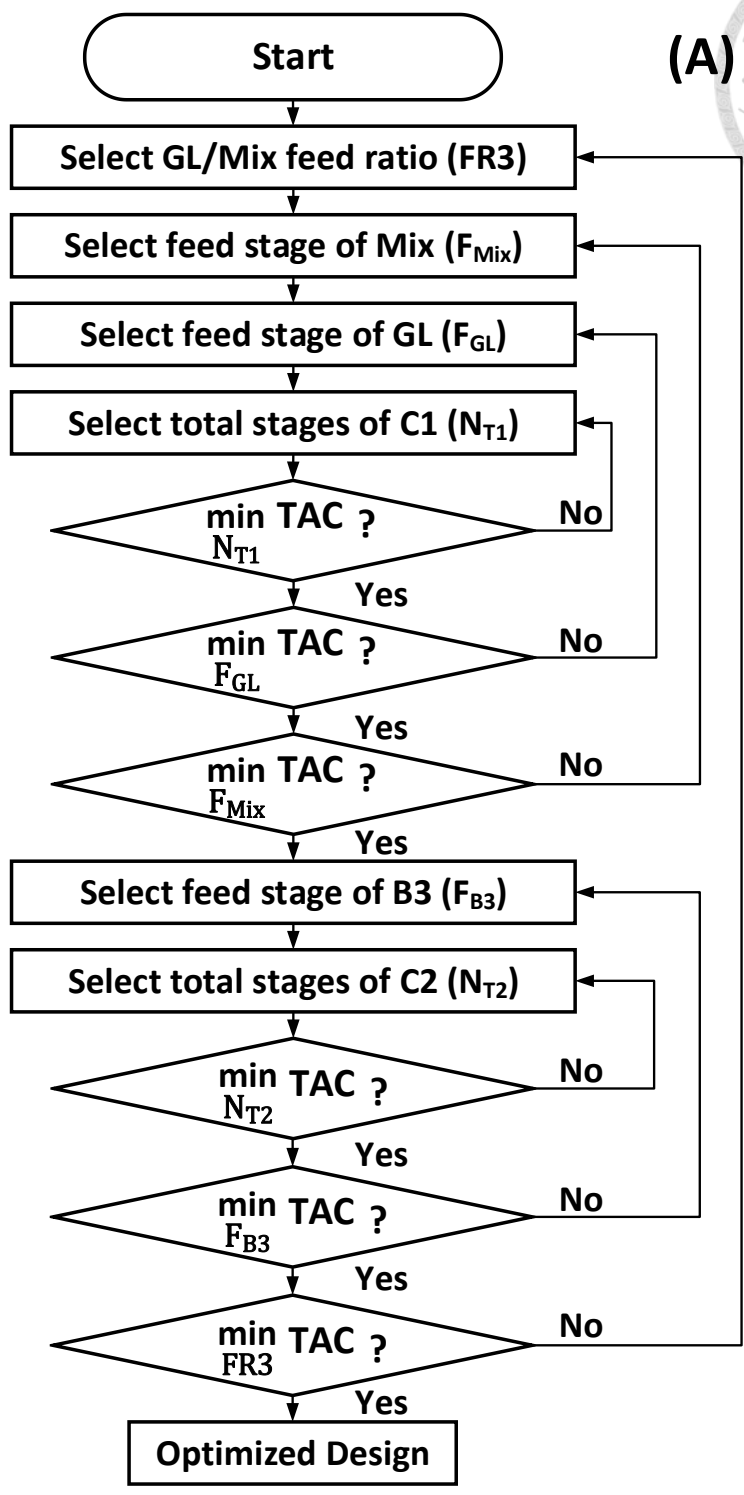


Figure 3-7 The optimization algorithm for reaction section, (A) RDC1; (B) RDC2



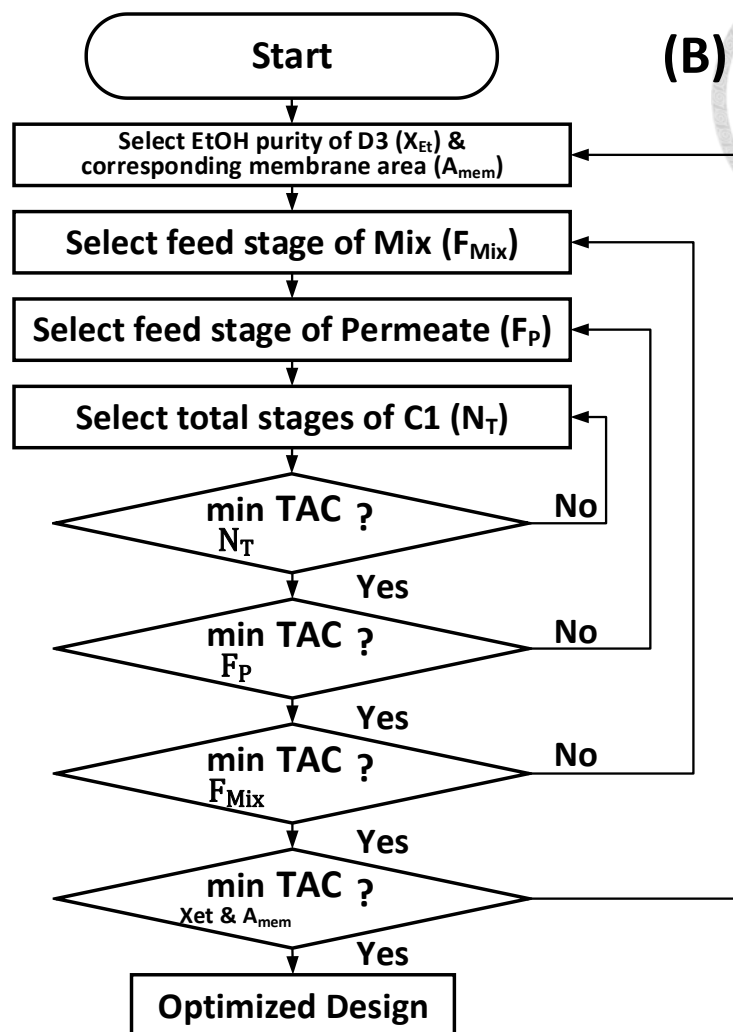
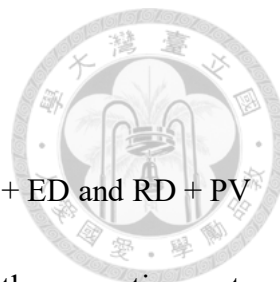


Figure 3-8 The optimization algorithm for separation section, (A) ED; (B) PV



#### 4. Results and Discussion

Before diving into the detailed optimization results between RD + ED and RD + PV systems. It is vital to clarify the optimal recycled EtOH purity from the separation part. This is because when the recycled EtOH purity decreases, the cost of separation would lower down. Conversely, the cost of the reaction part would increase. Moreover, the purity of EtOH recycled back to RDC1 could not be too small since it should be assured enough to carry out the reaction in the reactive distillation column. Hence, one should scrutinize this important trade-off first. Three different recycled EtOH purities (0.91, 0.95, and 0.99) have been studied.

Figure 4-1 shows the effect of recycled EtOH purity on TAC for both RD + ED and RD + PV systems. For the RD + ED system, the EtOH purity imposes slight influence on the TAC. It only declines from 500.94 to 494.36 (1000 USD) when the EtOH purity increases. The inverse correlation arises from the inherent characteristic of ED. To be more specific, EtOH is the lightest component in C1 thus it will come out as a distillate easily as glycerol is presented. Therefore, one can obtain a high purity of EtOH from D3. Nevertheless, when reducing the EtOH purity from D3, more energy needs to be applied to C1 to drives more H<sub>2</sub>O to the top. Last but not least, no matter which purity of EtOH is chosen, C2 must operate under atmospheric pressure to avoid cracking of glycerol. Therefore, the high cost of the vacuum system in C2 is irresistible as shown in Figure 4-

2.

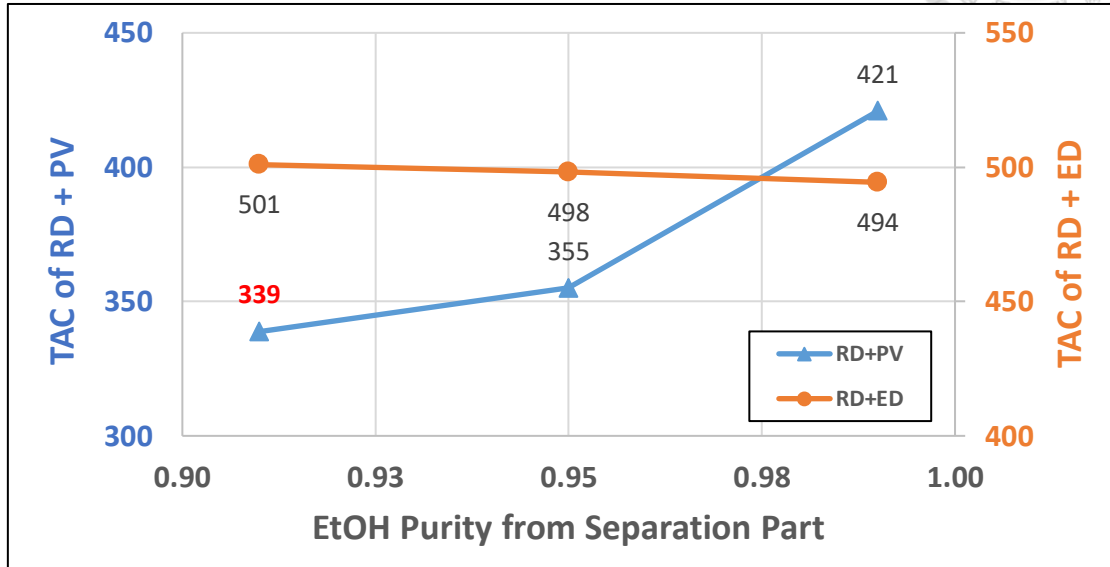


Figure 4-1 Effect of various recycled EtOH purity on TAC for RD + ED and RD + PV

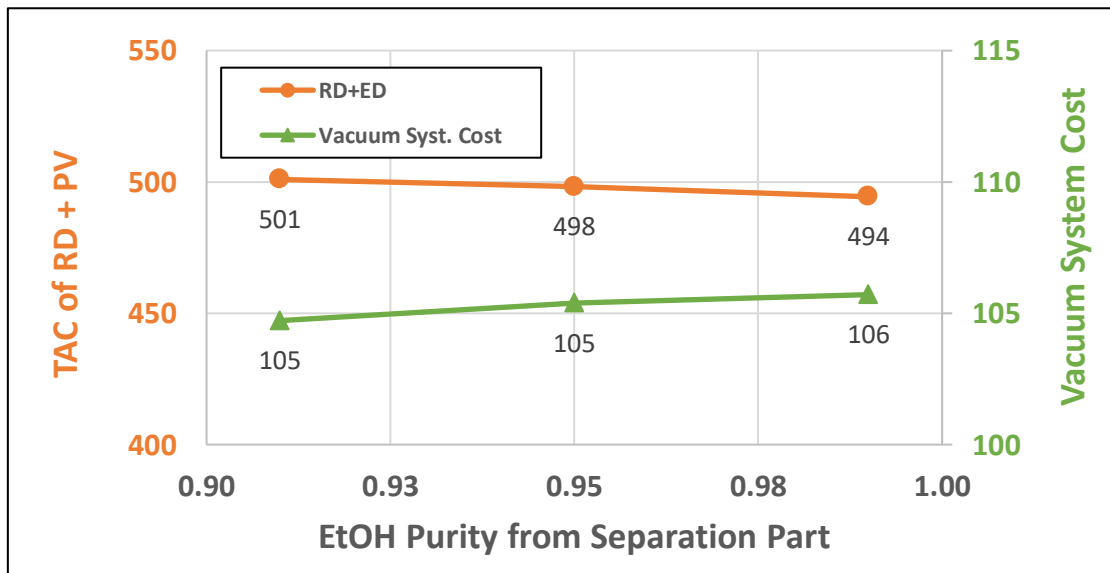
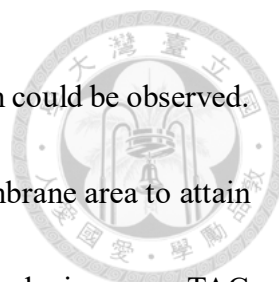


Figure 4-2 Effect of various recycled EtOH purity on vacuum system cost and TAC for

RD + ED



On the other hand, for the RD + PV system, a positive correlation could be observed. Explicitly speaking, when the purity rises, one requires far more membrane area to attain high purity EtOH. Especially, the phenomenon shows an exceedingly jump on TAC (355.04 to 420.87) from 0.95 to 0.99. The reason can be explained from Figure 4-3, as the purity increases, the cost of the membrane increases accordingly. Based on the investigation above, 0.99 and 0.91 are selected as the recycled EtOH purity for RD + ED and RD + PV, respectively.

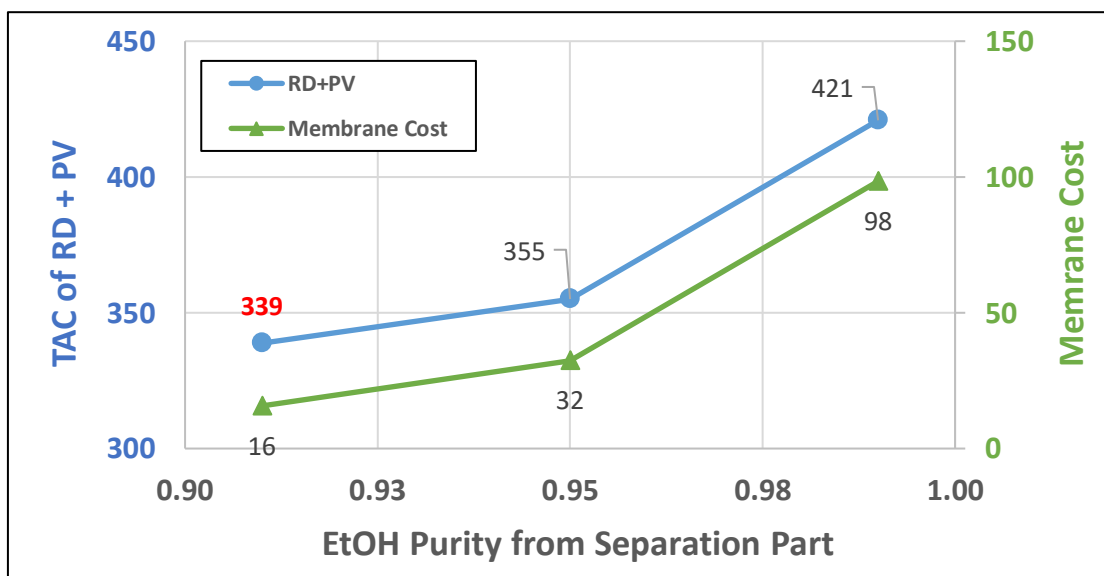
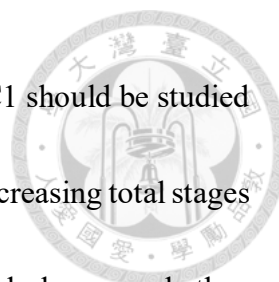


Figure 4-3 Effect of various recycled EtOH purity on membrane cost and TAC for RD +

PV



For the variables in RD + ED configuration, the total stages of C1 should be studied carefully. Figure 4-4 indicates the effect of total stages of C1. While increasing total stages of C1, the total implemental cost (TIC) of C1 increases in considerably larger scale than the total operating cost (TOC) of C2. Owing to the built-in identity of EtOH/H<sub>2</sub>O/Glycerol system, the entrainer performs well by separating EtOH from H<sub>2</sub>O under any stage of C1. This means that nearly trace amount of EtOH in B3 will go to C2, thus the TOC of C2 remains almost the same. In this case, the total stages of C1 are selected as 27.

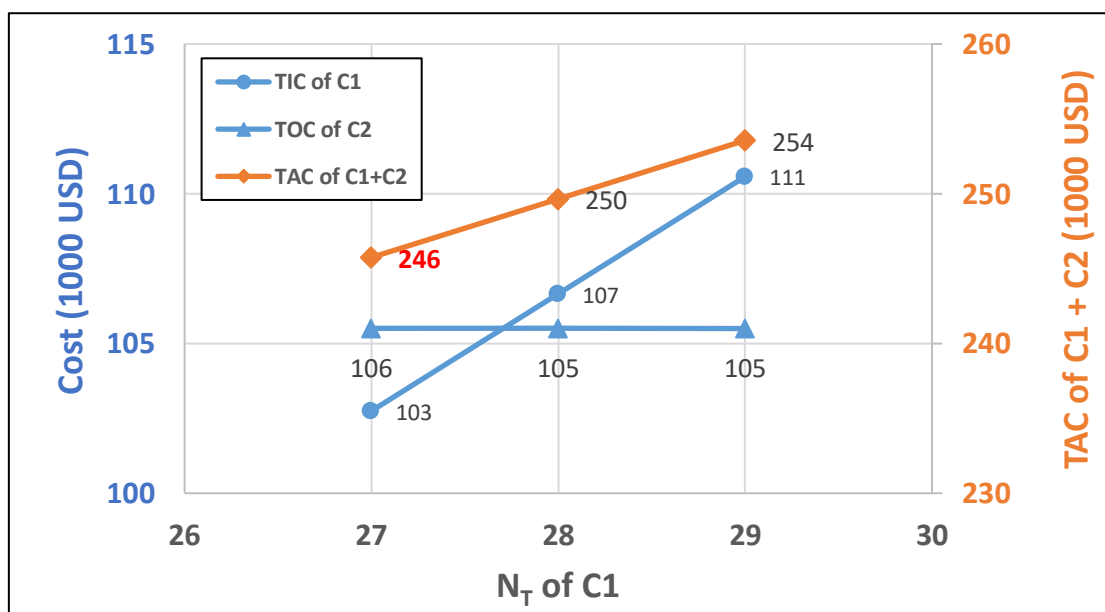
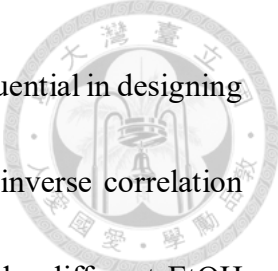


Figure 4-4 Effect of total stages of C1 on the cost of ED system



As for the configuration of RD + PV, the EtOH purity at D3 is influential in designing the parameters of C1 and pervaporation unit. Figure 4-5 shows the inverse correlation between the required membrane area and the reboiler duty of C1 under different EtOH purity at D3. As increasing the EtOH purity, a lot more energy is needed for obtaining high spec. of EtOH. On the contrary, less membrane area is required in this situation. Following the discussion above, Figure 4-6 demonstrates the membrane cost, TAC of C1, and TAC under various EtOH purity. The optimal EtOH purity that fed to the pervaporation unit is 0.83 since it achieves the lowest TAC.

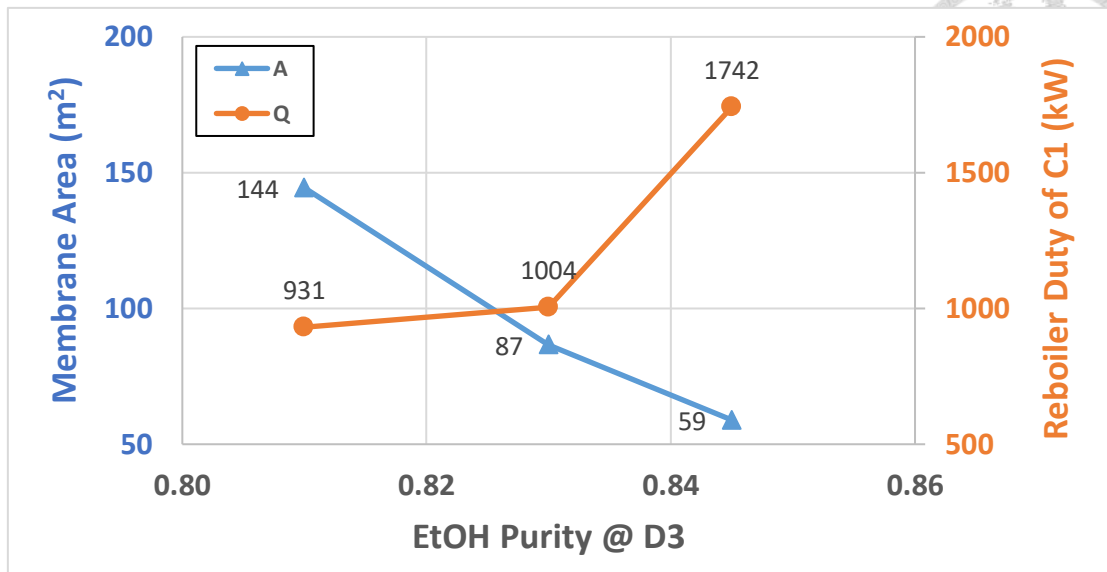


Figure 4-5 Effect of EtOH purity at D3 stream on reboiler duty of C1 and required membrane area

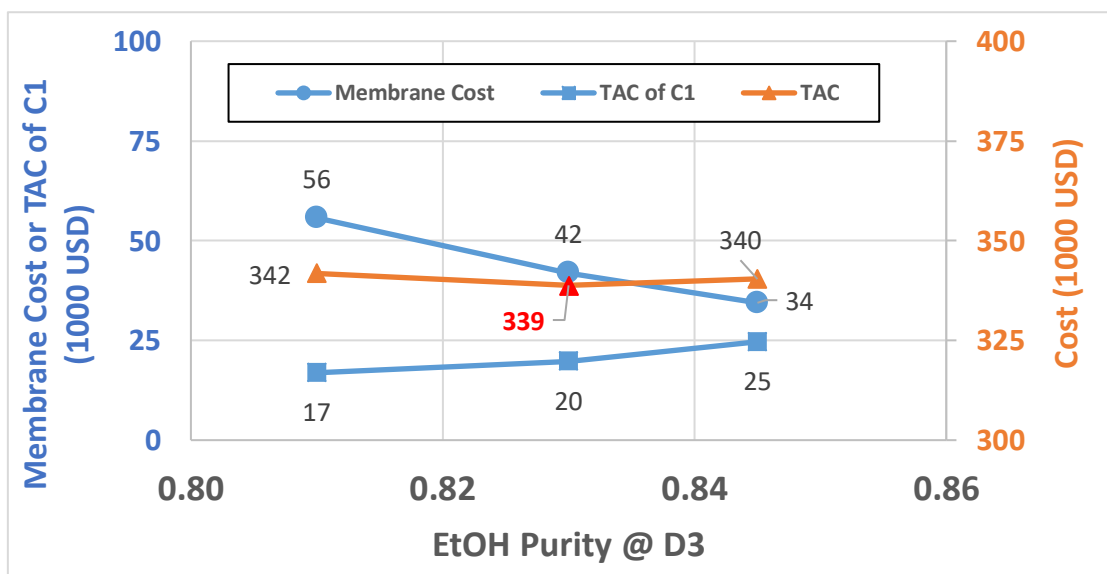


Figure 4-6 Effect of EtOH purity at D3 stream on the cost of TAC, TIC of C1, and membrane cost



Table 4-1 lists the detailed cost distribution of the RD + ED and RD + PV configuration. Compared to the separation part, in reaction part, the column has more stages to carry out both esterification and transesterification. Consequently, the cost for the reaction section is larger than separation section in both configurations. While investing in the operating cost in RD + ED, it is interesting to found that the cost of vacuum system almost made up of 74% of the operating cost. In other words, in order to prevent glycerol from losing its function, C2 must be operated under atmospheric pressure, which pays a lot in using ED. As for the configuration of RD + PV, the operating cost is just 2.70 (1000 USD). The considerable reduction can be contributed by the following factors. Firstly, by implementing the pervaporation unit instead of ED, only one column presents in the separation part. Hence, the capital cost is saved. Secondly, considering that the amount of molar flow fed to PV is not that large, the required membrane area is relatively small even if the cost for the membrane per square meter is high. Additionally, the steam/cooling water cost in both configuration includes the steam/cooling water utilized in distillation columns and heaters/coolers. To be more specific, the steam cost in the reaction section in RD + ED and RD + PV is quite high (18.34 and 24.98, separately). This is because in order to lower down the loading of the reboiler in RDC1, it is wise to preheat the EtOH feed stream. Furthermore, the cooling water cost in the separation section in RD + ED is about 17.03. The cost is mainly

generated from cooling down the entrainer stream to C1. In summary, by utilizing RD + PV configuration, all merits that possess will cause it to save effectively around 31.47% of TAC compared to RD + ED.



Table 4-1 Detailed cost distribution of RD + ED configuration

Payback period: 1/8	RD + ED				RD + PV			
	Reaction section		Separation section		Reaction section		Separation section	
	Capital	Operating	Capital	Operating	Capital	Operating	Capital	Operating
<b>Column</b>	286.25		43.37		257.94		16.68	
<b>Trays</b>	18.05		1.82		16.26		0.76	
<b>Reboiler</b>	0.05		0.47		0.04		0.18	
<b>Condenser</b>	0.06		0.15		0.05		0.16	
<b>Heater/ Cooler</b>	1.39		0.02		1.58		0.43	
<b>Feed Pump</b>	0.06				0.02		0.01	
<b>Vacuum Syst.</b>			0.24	105.47			0.24	0.67
<b>Catalyst</b>		0.93				0.58		
<b>Steam</b>		18.34		0.18		24.98		0.94
<b>Cooling water</b>		0.47		17.03		0.48		1.09
<b>Membrane</b>							15.71	
<b>Summary</b>	325.60		168.75		317.65		21.50	
<b>TAC</b>	<b>494.36</b>				<b>338.80</b>			

## 5. Conclusion



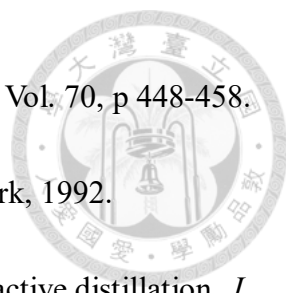
This research proposes a novel L<sub>1</sub>E production process consisting of two different separation configurations, namely extractive distillation and pervaporation. The process is targeting to synthesize 99 mol% L<sub>1</sub>E with EtOH and L<sub>1</sub> as reactants. For the reaction section, a stream has being side-drawing from RDC1 to acquire L<sub>1</sub>E product. Compared with the process concept by Miller et al.<sup>1</sup>, the advantage of adopting a side draw reduces the cost of another column for product purification. For the separation section, pervaporation intensifies the system appreciably more than extractive distillation since it decreases a tremendous amount of operating cost in the system. To illustrate, about 75.99% of operating cost in separation part and 31.47% of TAC are being saved. In conclusion, the RD + PV hybrid configuration is endowed with inherent economical-effective potential in terms of process intensification.

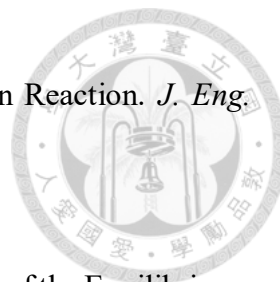
---



## Reference

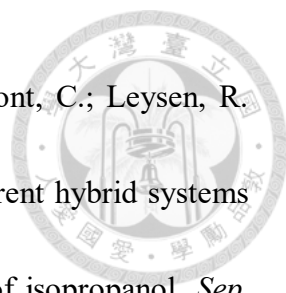
- (1) Miller, D. J.; Asthana, N.; Kolah, A.; Lira, C. T. Process for Production of Organic Acid Esters. US 7,652,167, Jan. 26, 2010.
- (2) Pereira, C. S. M.; Silva, V. M. T. M.; Rodrigues, A. E. Ethyl lactate as a solvent: Properties, applications and production processes - a review. *Green Chem.* **2011**, *13*, 2658-2671.
- (3) *Global Ethyl Lactate Market Research Report 2016*; Gos International Inc.: 2016.
- (4) de Jong, E.; Hisgson, A.; Walsh, P.; Wellisch, M. *Bio-Based Chemicals: Value Added Products From Biorefineries*; IEA Bioenergy, Task 42, Biorefineries: Wageningen, The Netherlands, 2013. (Available online at <http://www.ieabioenergy.com/wp-content/uploads/2013/10/Task-42-Biobased-Chemicals-value-added-products-from-biorefineries.pdf>)
- (5) Bidy, M. J.; Scarlata, C.; Kinchin, C. *Chemicals from Biomass: A Market Assessment of Bioproducts with Near-Term Potential*; National Renewable Energy Laboratory: Golden, CO, United States, 2016. (Available online at <http://www.nrel.gov/docs/fy16osti/65509.pdf>).
- (6) Asthana, N.; Kolah, A.; Vu, D. T.; Lira, C. T.; Miller, D. J. A Continuous Reactive Separation Process for Ethyl Lactate Formation. *Org. Process Res. Dev.* **2005**, *9*, 599-607.

- 
- (7) Doherty, M. F.; Buzad, G., *Reactive Distillation by Design*. 1992; Vol. 70, p 448-458.
- (8) Perry, R., *Chemical engineer's handbook*. McGraw Hill: New York, 1992.
- (9) Meirelles, A.; Weiss, S.; Herfurth, H. Ethanol dehydration by extractive distillation. *J. Chem. Technol. Biotechnol.* **1992**, *53*, 181-188.
- (10) Pinto, R. T. P.; Wolf-Maciel, M. R.; Lintomen, L. Saline extractive distillation process for ethanol purification. *Comput. Chem. Eng.* **2000**, *24*, 1689-1694.
- (11) Lynn, S.; Hanson, D. N. Multieffect extractive distillation for separating aqueous azeotropes. *Ind. Eng. Chem. Proc. Des. Dev.* **1986**, *25*, 936-941.
- (12) Arifin, S.; Chien, I. L. Design and Control of an Isopropyl Alcohol Dehydration Process via Extractive Distillation Using Dimethyl Sulfoxide as an Entrainer. *Ind. Eng. Chem. Res.* **2008**, *47*, 790-803.
- (13) Kober, P. A. Pervaporation, perstillation and percrystallization. *J. Membr. Sci.* **1995**, *100*, 61-64.
- (14) Lipnizki, F.; Field, R. W.; Ten, P.-K. Pervaporation-based hybrid process: a review of process design, applications and economics. *J. Membr. Sci.* **1999**, *153*, 183-210.
- (15) Waldburger Raoul, M.; Widmer, F. Membrane reactors in chemical production processes and the application to the pervaporation-assisted esterification. *Chem. Eng. Technol.* **1996**, *19*, 117-126.
- (16) Jyoti, G.; Keshav, A.; Anandkumar, J. Review on Pervaporation: Theory, Membrane



- Performance, and Application to Intensification of Esterification Reaction. *J. Eng.* **2015**, *2015*, 24.
- (17) Lee, H.-Y.; Li, S.-Y.; Chen, C.-L. Evolutional Design and Control of the Equilibrium-Limited Ethyl Acetate Process via Reactive Distillation–Pervaporation Hybrid Configuration. *Ind. Eng. Chem. Res.* **2016**, *55*, 8802-8817.
- (18) Gao, J.; Zhao, X. M.; Zhou, L. Y.; Huang, Z. H. Investigation of Ethyl Lactate Reactive Distillation Process. *Chem. Eng. Res. Des.* **2007**, *85*, 525-529.
- (19) Daengpradab, B.; Rattanaphanee, P. Process Intensification for Production of Ethyl Lactate from Fermentation-Derived Magnesium Lactate: A Preliminary Design. *Int. J. Chem. React. Eng.* **2015**, *13*, 407-412.
- (20) Hayden, J. G.; O'Connell, J. P. A Generalized Method for Predicting Second Virial Coefficients. *Ind. Eng. Chem. Proc. Des. Dev.* **1975**, *14*, 209-216.
- (21) Asthana, N. S.; Kolah, A. K.; Vu, D. T.; Lira, C. T.; Miller, D. J. A Kinetic Model for the Esterification of Lactic Acid and Its Oligomers. *Ind. Eng. Chem. Res.* **2006**, *45*, 5251-5257.
- (22) Su, C.-Y.; Yu, C.-C.; Chien, I. L.; Ward, J. D. Plant-Wide Economic Comparison of Lactic Acid Recovery Processes by Reactive Distillation with Different Alcohols. *Ind. Eng. Chem. Res.* **2013**, *52*, 11070-11083.
- (23) Luyben, W. L. Control of a Column/Pervaporation Process for Separating the

- 
- Ethanol/Water Azeotrope. *Ind. Eng. Chem. Res.* **2009**, *48*, 3484-3495.
- (24) Santoso, A. Design and Control of Hybrid Distillation-Membrane Systems for Separating Azeotropic Mixtures. Master thesis, National Taiwan University, Taiwan, 2010.
- (25) Tusel, G. F.; Brüscke, H. E. A. Use of pervaporation systems in the chemical industry. *Desalination* **1985**, *53*, 327-338.
- (26) Geankoplis, C., *Transport processes and separation process principles*. Prentice Hall Professional Technical Reference: New York, 1993.
- (27) Sert, E.; Atalay, F. S. n-Butyl acrylate production by esterification of acrylic acid with n-butanol combined with pervaporation. *Chem. Eng. Process. Process Intensif.* **2014**, *81*, 41-47.
- (28) Delgado, P.; Sanz, M. T.; Beltrán, S. Pervaporation of the quaternary mixture present during the esterification of lactic acid with ethanol. *J. Membr. Sci.* **2009**, *332*, 113-120.
- (29) Lee, F. M.; Pahl, R. H. Solvent screening study and conceptual extractive distillation process to produce anhydrous ethanol from fermentation broth. *Ind. Eng. Chem. Proc. Des. Dev.* **1985**, *24*, 168-172.
- (30) Douglas, J. M., *Conceptual design of chemical processes*. McGraw-Hill: New York, 1988.

- 
- (31) Van Hoof, V.; Van den Abeele, L.; Buekenhoudt, A.; Dotremont, C.; Leysen, R.  
Economic comparison between azeotropic distillation and different hybrid systems  
combining distillation with pervaporation for the dehydration of isopropanol. *Sep.*  
*Purif. Technol.* **2004**, *37*, 33-49.
- (32) Woods, D. R., *Cost Estimation for the Process Industries*. McMaster University:  
Hamilton, Ontario, Canada, 1983.
- (33) Oliveira, T. A. C.; Cocchini, U.; Scarpello, J. T.; Livingston, A. G. Pervaporation  
mass transfer with liquid flow in the transition regime. *J. Membr. Sci.* **2001**, *183*, 119-  
133.
- (34) Seider, W. D.; Seader, J. D.; Lewin, D. R.; Widagdo, S., *Product and process design  
principles: synthesis, analysis, and evaluation*. WILEY: New York, 2009.
- (35) Hooke, R.; Jeeves, T. A. "Direct Search" Solution of Numerical and Statistical  
Problems. *J. ACM* **1961**, *8*, 212-229.
- (36) Luyben, W. L., *Principles and Case Studies of Simultaneous Design*. WILEY: United  
States, 2011.

## Appendix



### A. Equation for Calculating the Equipment Cost

Most of the equations for calculating the cost are taken from Douglas and Seider et al. The payback period is set as 8 years as mentioned in the above context. The M&S Index is 1448.3 (2010, 1<sup>st</sup> quarter).

#### A-1 Equipment Sizing

##### A. Height of Column

$$L_c[ft] = 2.3 \times (N_T - 1) \quad (A-1)$$

where  $N_T$  is the total number of trays in the column.

##### B. Reboiler Heat Transfer Area

$$A_R[ft^2] = \frac{Q_R}{U_R \Delta T_R} \quad (A-2)$$

where  $U_R$  is 250 [BTU/(h\* $ft^2$ )].

##### C. Condenser Heat Transfer Area

$$A_C[ft^2] = \frac{Q_C}{U_C \Delta T_C} \quad (A-3)$$

where  $U_C$  is 150 [BTU/(h\* $ft^2$ )].



## A-2 Equipment Cost

### A. Cost of Column

$$\text{Column cost } [\$] = \frac{M\&S}{280} \times 101.9 \times D_c^{1.066} \times L_c^{0.802} \times (2.18 + 3.67) \quad (\text{A-4})$$

where  $D_c$  [ft] is the diameter of the column.

### B. Cost of Tray

$$\text{Tray cost } [\$] = \frac{M\&S}{280} \times 4.7 \times D_c^{1.55} \times L_c \times (1 + 2.18 + 3.67) \quad (\text{A-5})$$

### C. Cost of Heat Exchanger

$$\text{Heat Exchanger Cost } [\$] = \frac{M\&S}{280} \times A^{0.65} \times (2.29 + F_c) \quad (\text{A-6})$$

where  $F_c$  is 5.0625 and 3.75 for reboiler and condenser, respectively.

### D. Cost of Membrane Material<sup>31</sup>

$$\text{Membrane Material Cost } [\$] = \frac{475.0}{m^2} \quad (\text{A-7})$$

### E. Cost of Membrane Module<sup>24</sup>

$$\text{Membrane Module Cost } [\$] = 125550 \times \left(\frac{A}{324}\right)^{0.3} \quad (\text{A-8})$$

where  $A$  [m<sup>2</sup>] is the membrane area for each module.



## F. Cost of Vacuum system

### RD + ED system:<sup>34</sup>

$$\text{Steam – Jet Ejector Cost } [\$] = \left(\frac{CE}{500}\right) \times 1690 \times S^{0.41} \quad (\text{A-9})$$

where CE is the cost index;  $S = \frac{\text{Flow rate } [\text{lb/hr}]}{\text{Pressure } [\text{torr}]}$  is the size factor.

### RD + PV system:<sup>32</sup>

$$\text{Vacuum Pump Cost } [\$] = 4200 \times \left(\frac{60 \times F_P \times 8.314 \times 273.15}{3600 \times 101.325}\right)^{0.55} \quad (\text{A-10})$$

where  $F_P$  is the total permeate rate through the membrane [kmol/hr].

## G. Cost of Feed Pump<sup>32</sup>

$$\text{Feed Pump Cost } [\$] = 26700 \times \left(\frac{24 \times 3600 \times F_F}{50000}\right)^{0.53} \quad (\text{A-11})$$

where  $F_F$  is the total feed rate to the pump [m<sup>3</sup>/s].



### A-3 Operating Cost

#### A. Steam and Cooling Water Cost<sup>30</sup>

$$\text{Annual Cost of the Steam} = \frac{2.8}{1000} \times \frac{Q_H}{912} \times 8150 \quad (\text{A-12})$$

$$\text{Annual Cost of the Cooling Water} = \frac{0.03}{1000} \times \frac{Q_C}{912} \times 8150 \quad (\text{A-13})$$

#### B. Power of Vacuum System<sup>33</sup>

$$\text{Annual Cost of Power} = 8150 \times 0.04 \times \left\{ \left( \frac{F_P \times 8314 \times T}{3600} \right) \left( \frac{k_r}{k_r - 1} \right) \left[ \left( \frac{1.013}{P_{Op}} \right)^{\frac{k_r - 1}{k_r}} - 1 \right] \right\} \quad (\text{A-14})$$

where  $k_r$  is heat capacity ratio;  $P_{Op}$  is the pressure on the permeate side.

#### C. Chilled Water Cost<sup>36</sup>

In this study, the permeate side is under the 0.16 bar. In order to cool it to the liquid, the usage of chilled water is necessary which is \$4.43/GJ.

#### D. Catalyst Cost (assuming a catalyst life time of 3 months)

$$\text{Catalyst Cost } [\$] = \text{catalyst loading } [kg] \times 7.7162 \frac{\$}{kg} \quad (\text{A-14})$$